MULTIOBJECTIVE OPTIMIZATION OF HEAT EXCHANGER DESIGN GEOMETRY: AN APPLICATION OF EVOP

A Thesis Submitted
in Partial Fulfillment of the Requirements
for the Degree of

MASTER OF TECHNOLOGY

March, 2000

by

MAYUR MANOHAR DHANDARPHALE

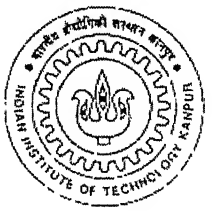

DEPARTMENT OF INDUSTRIAL AND MANAGEMENT ENGINEERING
INDIAN INSTITUTE OF TECHNOLOGY
KANPUR – 208016 (INDIA)

CERTIFICATE

It is certified that the work contained in the thesis entitled, "MULTIOBJECTIVE OPTIMIZATION OF HEAT EXCHANGER DESIGN GEOMETRY: AN APPLICATION OF EVOP" by *Mr. Dhandarphale Mayur Manohar* has been carried out under our supervision and that this work has not been submitted elsewhere for a degree.

Dr. Gautam Biswas
Professor
Department of Mechanical Engineering,
Indian Institute of Technology, Kanpur.

Dr. Tapan Bagchi
Professor
Department of Industrial and
Management Engineering,
Indian Institute of Technology, Kanpur.

March, 2000

ACKNOWLEDGEMENT

I wish to express my deep sense of gratitude and indebtedness towards Dr. T. P. Bagchi as well as Dr. Gautam Biswas for his inspiring guidance, invaluable suggestions and constructive criticism. They were always a constant source of encouragement throughout my thesis work.

I am very much thankful to Mr. Ashish Kulkarni for his support to me. I heartily appreciate the keen interest shown by Pankaj, Anshuman, Sudhir and Murali in the IME lab and their help to me. I also would like to thank Yogesh, Swapnil, Girish and Amod for their invaluable encouragement. I will miss them forever.

I would like to thank my ghatmandal friends for making my stay at IITK very enjoyable. I thank all those who have contributed directly or indirectly to my thesis.

CONTENTS

Requirements of small-size and lightweight heat exchanger devices in power, space, process and aerospace industries have resulted in the development of specially designed heat transfer surfaces. However, in most practical cases, the heat transfer coefficients are low. In order to enhance heat transfer between the flowing fluid and closely spaced parallel plate channels, in the case of plate-fin heat exchangers, protrusions can be mounted on the channel surfaces. The protrusions in the form of winglet-type vortex generators are capable of enhancing heat transfer at the expense of relatively small increase in pressure penalty as compared to other protrusions geometries.

To maximize *heat transfer* while incurring minimum *pressure penalty* is an important design goal and this is the primary objective of the present investigation. To evaluate different heat exchanger geometries this study utilizes the MAC (Marker and Cell) algorithm. A three-dimensional numerical model of this algorithm is used to solve full Navier-Stokes equations together with the governing equations for energy conservation in a rectangular channel with a built-in winglet vortex generator.

For the bi-criteria optimization of heat exchanger design geometry, multiple criteria optimization methods may be used. This study has appraised the usefulness of EVOP for solving multi-objective engineering design problems for which GA (Genetic Algorithms) or other multi-objective methods cannot work due to practical limitations. EVOP is a simple but powerful technique, created by Box and Draper (1969), which has been widely and successfully used in empirical process optimization in a variety of process industries.

This work has demonstrated that EVOP can be an effective method to find Pareto Optimal engineering designs particularly when the number of design evaluations performed must remain small in number.

List of Figures

Figure No.	Title	Page No.

List of Tables

1. Introduction

1.1 A Heat Exchanger Design Problem

Requirements of small-size and lightweight heat exchanger devices in power, process and aerospace industries have resulted in the development of specially designed heat transfer surfaces. It is possible to distinguish different basic flow configurations, such as internal flow through tubes, external flow normal to the tubes and channel flows in a wide range of heat exchangers. In most practical cases, the heat transfer coefficients for the configuration of flow over flat surfaces are significantly low. In order to enhance heat transfer between the flowing fluid and closely spaced parallel plate channels, in the case of plate-fin heat exchangers, protrusions can be mounted on the channel surfaces. The protrusions in the form of slender delta wing or winglet-type vortex generators are capable of enhancing heat transfer at the expense of relatively small increase in pressure penalty as compared to other protrusion geometries.

Experimental investigations reveal enhancement of heat transfer in the presence of longitudinal vortices. Such vortices are characterized by their rotating motion and longevity. (Biswas et al. 1995)

Computational studies on related topics have been performed by Fiebig and Biswas (1989) and Chattopadhyay (1992) in a geometrical configuration of delta wing placed inside a rectangular channel. Both studies confirm significant transport enhancement. In another recent study, Biswas *et al.*(1994) have determined that winglets are a more attractive choice than delta wings as vortex generators for enhancing heat transfer.

The present study is aimed at a numerical investigation of heat transfer enhancement while incurring minimized pressure penalty in a channel with a built-in winglet type vortex generator placed in a fully developed laminar flow. Since this study utilizes the state-of-art MAC (Marker and Cell) algorithm to do design evaluation with each evaluation taking 3-4 hours on a SGI Origin 200 (4 Mips R10000 processor, 512 MB Ram, 30 GB HDD, 10/100 Ethernet Interface machine), GA- based multi-objective methods such as ENGA (Bagchi, 1999) could not be used here. Rather, we adopted a variation of the EVOP method described below for this purpose.

1.2 EVOP Technique for Optimization

1.2.1 Theoretical Foundation of EVOP

Over the course of its life a typical industrial process passes through many stages of development. When a plant is built, it ideally incorporates the best design possible, given the available knowledge and resources. Nevertheless the process of 'tuning' still remains to be done to improve quality, yield, cost, performance, cycle time etc.

Consequently in most industrial organizations considerable effort is made to further improve the process after its start-up. In addition to the recording and examination of routine plant data, special studies are frequently carried out in the laboratory, on the pilot plant, and also on the full-scale process by the research and development staff. Such investigations, particularly when they employ efficient modern investigatory tools of statistical design and analysis, are most valuable and must continue (Box and Draper, 1969).

The shortage of technical personnel however inevitably limits the amount of special investigation of this kind. There is a special technique that makes only sparing use of technical manpower and complements the special investigations already referred to. Fig.(1.1) shows the typical improvement in productivity with the use of EVOP technique as compared to the productivity improvement with normal technical effort alone. (Box and Draper, 1969).

Because of the continual technical effort exerted on process improvement, we normally find a steady increase in productivity. From one point of view, one does not know at the beginning of any particular time which particular processes will be improved or what the precise nature of the improvements will be but, nevertheless, one can predict with some exactitude what the overall effect of applying his technical work will be. From another point of view, the near certainty of the specific amount of process improvement expected during the forthcoming year may be depressing. One knows that without some new initiative he cannot hope to increase the rate of improvement of productivity.

There is a simple but powerful empirical technique, that extends one such initiative. Created by Box and Draper (1969) it is called Evolutionary Operation or more briefly,

EVOP. It has now been widely and successfully used in the chemical industry, but would undoubtedly be of value in other types of manufacture as well. The present study is an attempt to use EVOP to find Pareto optimal heat exchanger designs.

Evolutionary Operation is really a management technique in which a continuous routine becomes the basic mode of operation for the plant and replaces normal static operation. Evolutionary Operation is not a substitute for fundamental R & D investigation. Rather, such investigation should use full factorial experiments (DOE) and should continue side by side with EVOP. Evolutionary Operation does, however, often indicate areas to which more fundamental approaches such full-fledged DOE could usefully be directed.

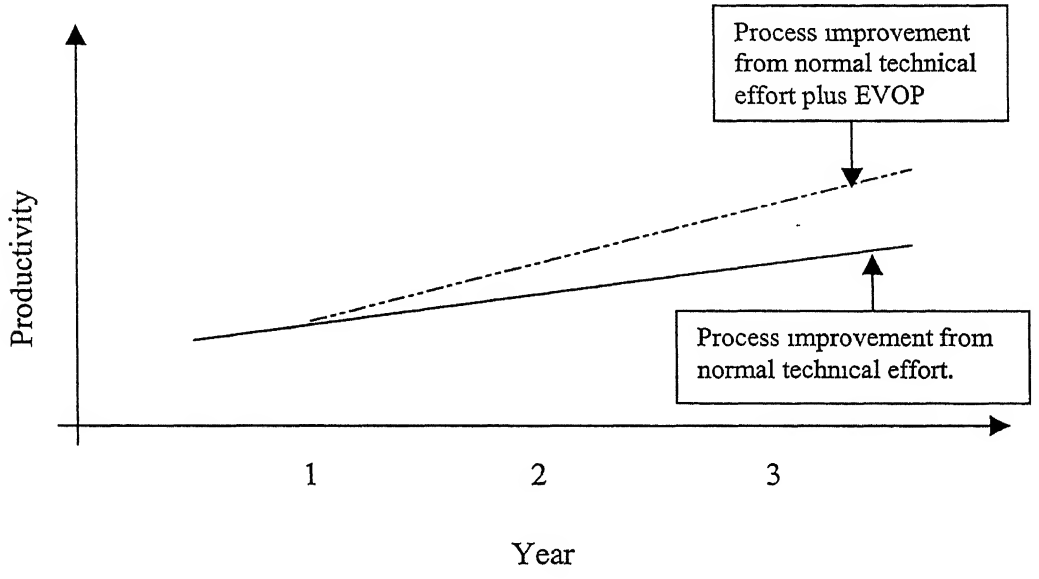

Figure 1.1: Productivity improvement with EVOP technique

In the EVOP method a carefully planned *cycle* of *minor* variants on the process is agreed upon by those seeking to improve the process. The routine of EVOP consists of running each of the variants in turn and continually repeating the cycle. The cycle of variants follows a simple pattern, the persistent repetition of which allows evidence concerning yield and physical properties of the product in the immediate vicinity of the works process to accumulate during routine process runs. In this way we use routine process running to generate not only the product we require for business but also the information we need to improve it.

Controlled variations thus being introduced into the process, the effect of *selection* is introduced by arranging for the results to be continuously presented. The stream of information concerning the outputs from the various process conditions is summarized. The information is set out in such a way that the analyzer can at any time see what weight of evidence exists for moving the center of scheme of variants to some new point, what types of changes are undesirable from the standpoint of producing results of inferior quality, how much the scheme is costing to run, and so on.

In making permanent change in the routine of process, the situation is very different from that which we meet in running specialized experiments such as those using DOE (Design of Experiments). The latter will last a limited time, during which special facilities can be made available. Evolutionary Operation, however, is virtually a permanent method of running the process. Changes in the levels of the variables can be permitted whose effects are virtually undetectable in individual runs, and only techniques simple enough to be run continuously by works personnel themselves under actual conditions of manufacture can be employed.

Suppose a new plant has just been built. We imagine the improvements, which could arise from suitable adjustments to the new process measured on some scale such as profitability and arranged in a descending order of magnitude. (Refer Fig. 1.2)

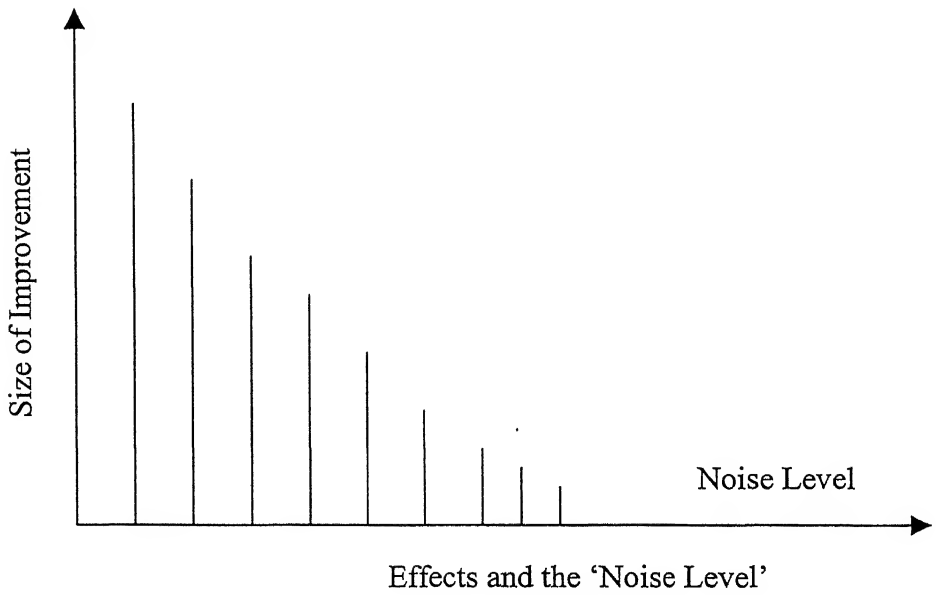

Figure 1.2: Size of improvement and Noise level

A few very large effects to the left of the diagram will be quickly detected after startup. Their causes will then be tracked down and adjustments and improvement of the process will result.

The reason that these effects can be rapidly detected, hence, exploited, is that the 'signal' they produce is large compared with the underlying level of variation of the process, sometimes called 'noise level'.

Noise arises from a variety of sources such as variability of raw materials, inability to maintain precisely input variables at set levels, and from instrument and measurement error. Such variation is often regarded as inherent.

To discover effects buried in noise we must improve the signal-to-noise ratio. We must either decrease the effective noise level or increase the signal level. In EVOP we do both. The signal is deliberately increased by introducing changes of a *carefully chosen kind* in the process conditions or variables under study. Repetition of the changes and averaging of the results reduce the effective noise level.

1.2.2 An Example of EVOP

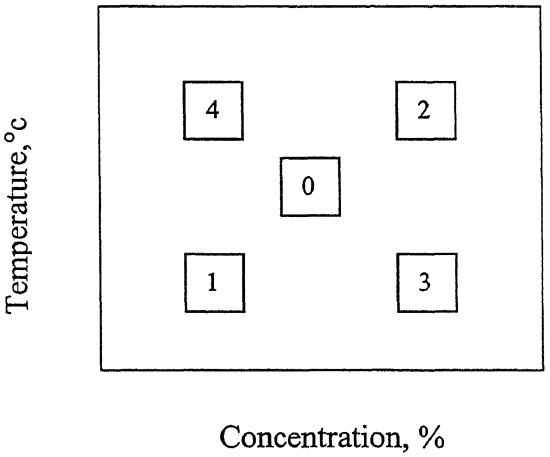

Figure 1.3: Controlled Variation in Design Inputs

The variables under study

At a particular stage of a development of a certain batch process, two process variables or factors were being studied. These were, respectively, the percentage concentration of a

certain feed material and the temperature at which the reaction was conducted.

A Pattern of Variants of Design

The scheme of variants is shown in above figure. The *current* works process is labeled '0' and the four variants are labeled 1,2,3, and 4. One batch of product was made at each set of conditions, which were run successively in the order 0,1,2,3,4; 0,1,2,3,4; and so on.

Responses of Interest

Three responses were recorded:

1. The cost of manufacturing unit weight of product.
2. The percentage of a certain of impurity.
3. A measure of fluidity.

The Information Board

The information was displayed on a "board". The essential thing is that this information (data) and its display should be simple. In general, the information should consist of cycle number, phase number and the output (response) factors in figures.

Analysis of the Information Board

After studying the information board and combining the ideas it conveys with production requirements and his special knowledge of the process, the superintendent can make one of two basic decisions:

1. To allow the scheme to proceed unchanged and wait for additional information from the next cycle.
2. To modify operation in some way, so beginning another phase of the EVOP scheme.

Under alternative 2, a number of possibilities are available. Some of these are as follows:

- Adopt one of the evolved
- variants as the new 'works process' and recommence the cycle about this new center point.

- Explore an indicated favorable direction of advance and recommence the cycle about the best condition found.
- Substitute new variables for one or more of the old variables.
- Modify the pattern of variables for one or more of the old variables waiting to be tested on the EVOP scheme.

We can see from this example that the actions to be taken in various circumstances are not precisely specified. Human judgement is a very important part of an EVOP investigation as it should be any investigation. A properly run EVOP scheme ensures that the process out of the hands of the process superintendent is continuously fed with clear information about this process on which he then takes what actions he deems appropriate. Although there are certain principles in this game, judgement is called for at every stage to evaluate the possibilities of future success or failure and to act accordingly.

1.3 Multi-Objective Optimization

Many real world problems involve multiple measures of performance, or objectives, which should be optimized simultaneously. In certain cases, objective functions may be optimized separately from each other and insight gained concerning the best that can be achieved in each performance dimension. However, suitable solutions to the overall problem can seldom be found in this way. Optimal performance according to one objective, if such an optimum exists, often implies unacceptably low performance in one or more of the other objective dimensions, creating the need for a compromise to be reached (Fonesca and Fleming, 1995). A suitable solution to such problems involving conflicting objectives should offer 'acceptable', though possibly sub-optimal in the single-objective sense, performance in all objective dimensions, where 'acceptable' is a problem-dependent and ultimately subjective concept.

1.4 Multiple Criteria Decision Making

Decision making is the selection of an act or courses of action from among alternative acts or courses of actions such that it will produce optimal results under some criteria of

optimization (Tabucanon, 1989). This concise definition of decision making invokes further elaboration to a certain extent. Before the problems can be considered well defined, the set of alternatives and the set of criteria have to be known and established first; only then can the selection process commence. What makes multiple criteria decision-making complex is the *plurality* of the criteria involved in the problem. In decision analysis of complex systems, such terms as 'multiple criteria', 'multiple objectives', or 'multiple attributes' are used interchangeably to describe decision situations while there are no universal definitions of these terms. *Multiple criteria decision-making* (MCDM) has seemed to emerge as the accepted nomenclature for all models and techniques dealing with multiple objective decision making or multiple attribute decision making.

An example of the Multiple Criteria Decision Making

Production Planning involves the following multiple objectives:

Max{Total net revenue}

Max{Minimum net revenue in any period}

Min{Backorders}

Min{Overtime}

Min{Finished goods inventory}

Such multiplicity of criteria occur in almost every area of business decision making and operations. They appear in accounting, finance, operations management, manpower planning etc.

The general multi-objective problem requiring the optimization of k objectives may be formulated as follows:

Max (min) $Z_j = f_j(X)$, j=1,2,…,k

Subject to

- $g_i(X) \leq b_i$, i = 1,2,…,m
- $X \geq 0$

where X is a vector of decision variables and $g_i(X)$ are the inequality constraints. In multi-criteria optimization, because the objectives are often conflicting, there does not exist a single unique solution, which is globally optimum with respect to all the conflicting objectives. The increment in any of these objectives will decrease the others and vice versa.

A necessary condition of MCDM is the presence of *more than one* criteria. The sufficient condition is that the criteria must be *conflicting* in nature. In summary, a problem can be considered as that of MCDM if and only if there appears at least two *conflicting* criteria and there are at least two *alternative* solutions (Tabucanon, 1989).

Criteria are said to be in conflict if the full satisfaction of one will result in impairing or precluding the full satisfaction of the other(s). The criteria are considered to be 'strictly' conflicting if the increase in satisfaction of one results in a decrease in satisfaction of the other. The sufficient condition of MCDM, however, does not necessarily stipulate 'strictly' conflicting criteria.

In view of the conflicting nature of the criteria involved in MCDM, choosing the 'best' alternative is indeed a difficult task for the decision-maker. Consequently there is a need for methods to systematically resolve the conflicts among criterion (or objectives) in order to reach acceptable compromises and make up with satisfying (or termed as 'satisficing') solutions.

1.5 The Concept of Pareto Optimality

A special "family" of solutions of a multi-objective optimization comprises all those elements of the search space which are such that the components of the corresponding objectives vectors cannot be all simultaneously improved. In economics such solutions are called Pareto optimal.

A more formal definition of Pareto optimality is as follows (Tabucanon, 1989):

Consider, without loss of generality, the minimization of the n components f_k, $k = 1,\ldots,n$, of a vector variable x in a universe U_x is said to be Pareto optimal if and only if there is

no $x_v \in U_x$ for which $v = f(x_v) = (v_{1,..}, v_n)$ *dominates* $u = f(x_u) = (u_1, , u_n)$, i.e., there is no $x_v \in U_x$ such that

$\forall i \in \{1,...n\}, v_i \leq u_i \cap \exists_i \in \{1,...,n\} | v_i < u_i$

The set of all Pareto-optimal decision vectors is called the *Pareto optimal, efficient,* or *admissible set* of the solutions. The corresponding set of objective vectors is called the *non-dominated* set. In practice, however, it is not unusual for these terms to be used interchangeably to describe solutions of a multi-objective optimization problem.

In Fig.1.4, the Pareto optimal set of solutions is shown by dark points on the dotted line, which are solutions numbered 10, 11,8 and 7.

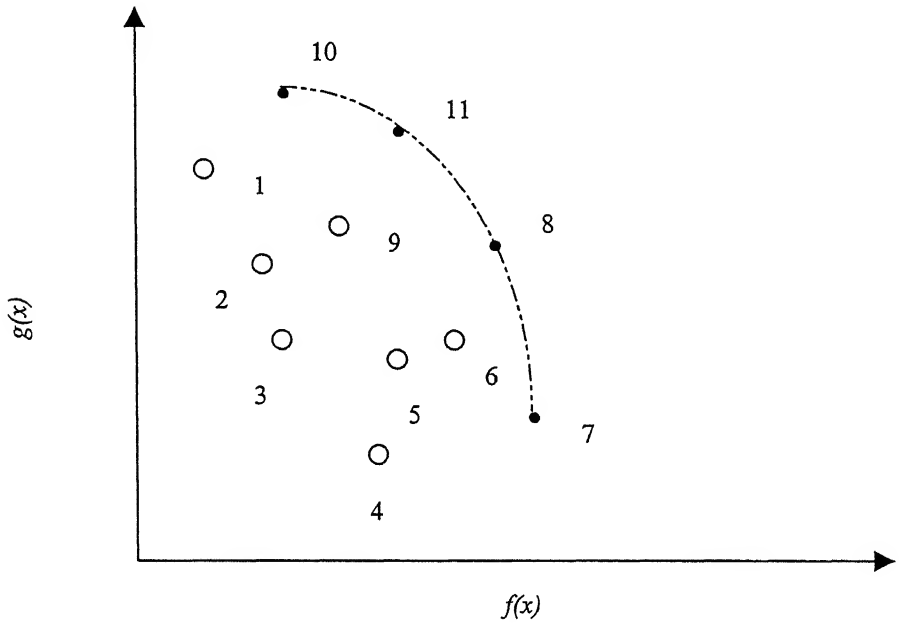

Figure 1.4:The Efficient Front in Bi-objective Maximization Problem

The notion of Pareto Optimality is only a first step towards the practical solution of a multi-objective problem. This decision involves selecting subsequently a single compromise solution from the non-dominated set according to some preference information. All other solutions are dominated in the Pareto sense and they may be ignored.

Finding Pareto optimal solutions, however, is not straight forward. Recently, methods based on metaheuristics have been suggested (Srinivas and Deb, 1995; Bagchi, 1999). The present work is an attempt to use EVOP when such methods would not be practicable.

2. Problem Definition

2.1 Description of the Problem

2.1.1 Introduction to Heat Exchanger Design

Fin-tubes are generally used in gas-liquid heat exchangers where the gas is in the crossflow to the tubes and the liquid flows inside the tubes. Figure (2.1) shows the arrangement of the core region of a fin-tube crossflow heat exchanger. The purpose of the fin is to enhance the heat transfer coefficient on the gas side to a value comparable to the liquid side. The area ratio of the fins to the tubes varies depending on the application and may reach a value of 30. Plate-fin heat exchangers also find application in many industrial processes. Such heat exchangers may be used to exchange energy between two different gases or liquids. Figure (2.1) illustrates the basic arrangement of the core region of a plate-fin heat exchanger. In forced convection heat transfer between a gas and a liquid, the heat transfer coefficient of the gas may be 10 to 50 times smaller than that of the liquid. In order to increase the heat transfer on the gas side, the fin geometry can be manipulated (Webb, 1987) in various ways. In addition, compactness of the heat exchangers is demanded for effective utilization of energy and to bring about a save on material and space. The performance of heat exchanger surfaces brings about a save on material and space. The performance of heat exchanger surfaces can be enhanced by mounting protrusions on the surfaces. The offset strip-fin and the louvered fins have been widely used for this purpose (Webb, 1987). The basic mechanism involved in the above mentioned cases is the periodic interruption of the boundary layer by separation, wake recovery and generation of thin developing boundary layer with high Nusselt Number.

A somewhat different concept for the reduction of the thermal resistance is to induce longitudinal streamwise vortices in the flow field. The longitudinal vortices can be generated by mounting delta wing or winglet type vortex generators on the flat surfaces (Fig. 2.1). The longitudinal vortices develop along the side edge of the wing-shaped vortex generator due to the pressure difference between the front surface facing flow and the back surface. These streamwise vortices interact with an otherwise two-dimensional

boundary layer and produce a three dimensional swirling flow that mixes near wall fluid with the free stream. This mechanism strongly enhances the exchange of fluid between

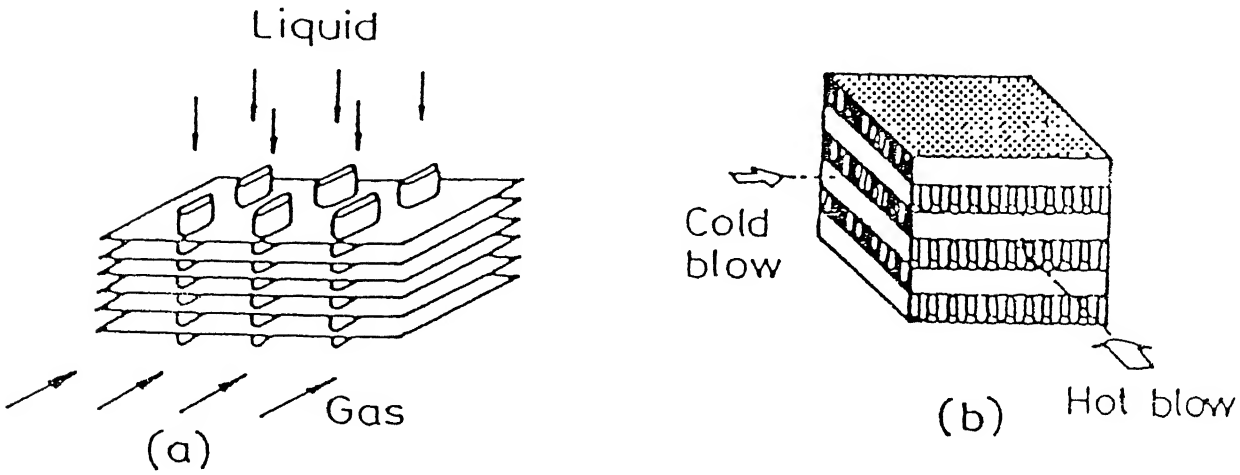

Figure (2.1): Typical arrangement of heat exchanger cores (a)Gas-liquid fin-tube cross-flow (b) Plate fin (single or multi pass)

the wall and the core region of the flow field, which causes high heat transfer augmentation. The additional pressure lasses are modest because the form drag for such wing-type slender bodies is low. A complete numerical evaluation of heat transfer in a fin-tube or plate-fin crossflow heat exchanger would be extremely difficult. In order to understand the basic mechanisms involved in enhancement of heat transfer and to evaluate the performance parameters quantitatively, a need is felt to analyze three-dimensional flow and heat transfer in a horizontal channel with built-in vortex generators. A number of experimental investigations (Edwards and Alker, 1974; Russel *et al.*, 1982, Fiebig *et al.*, 1986) in fields relevant to the present problem have been reported in the literature. Computational studies on related topics have been performed by Fiebig *et al* (1989) and Biswas and Chattopadhyay (1992) for laminar flows.

2.1.2Enhancement of Heat Transfer by mounting protrusions on surfaces

The subject of enhanced heat transfer is of serious interest in heat exchanger applications. Concepts like space and energy optimization in power and process industries call for more and more compact designs of heat exchangers. Specially designed surfaces use protrusions mounted on them to enhance heat transfer. Some typical examples of the enhanced heat transfer surfaces which are very popular in different industrial applications (Webb, 1987) are shown in Fig. (2.2). There have been a number of recent survey articles and handbook sections (Bergles, 1978, 1983, 1985). Special surface geometries bring about the transport-enhancement by establishing a higher "**hA**" per unit base surface area. It may be mentioned that (1/hA) is the thermal resistance associated with heat transfer by convection at a surface. Some well-known methods of manipulation of surface-geometry are:

1. Inserting twisted tapes or turbulence promoters for internal flows in circular tubes.
2. Roughening the surfaces for channel flows in closely spaced parallel plate channels, typical of plate-fin and plate type heat exchangers.
3. Improving flow structure in external flows normal to tubes and tube banks.

2.1.3 Flows in Parallel Plate Channels Formed by Two Neighboring Fins of Plate-Fin or Fin-Tube Heat Exchangers

It may be mentioned here that we are particularly interested in enhancement of heat transfer in the gas side of fin-tube heat exchangers (with flat fins) and enhancement of heat transfer in plate-fin heat exchangers. With this intent, we would like to study different investigations related to augmentation of heat transfer suitable for proceeding applications.

Augmentation of heat transfer is of special interest in channel flows where the rate of the heat transfer between the fluid and the channel walls deteriorates as the boundary layer grows on the channel walls and the flow tends to become fully developed. Protrusions can be mounted on these channel walls in order to disrupt the growth of the boundary layer and thereby enhance the heat transfer between the flowing fluid and the channel walls. Two relevant applications using this kind of flow configuration are the heat trans

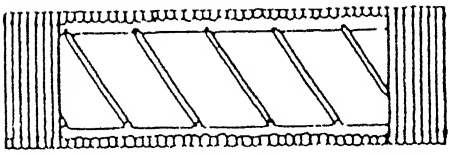

(a)

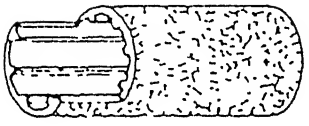

(b)

P_t = Axial distance through which the tape is twisted by 180°

Twist ratio
$r_t = p_t / 2d_i$

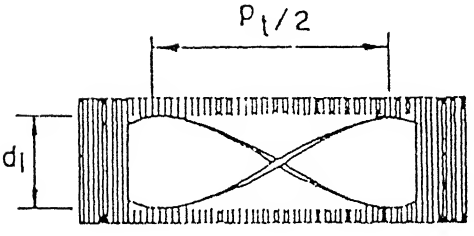

(c)

Figure 2.2 Various methods of making enhanced tubes: (a) helical rib on inner surface and integral fin on outer surface (b) internal fins on inner surface and porous coating on other surface (c) twisted tape insert on inner surface and integral fins on outer surface.

fer between the gas and the fin in the case of gas-liquid fin-tube cross-flow heat exchangers and the heat transfer between flowing fluid and plates in the case of plate-fin heat exchangers (Fig.2.3). The evolution towards a fully developed flow can be disturbed

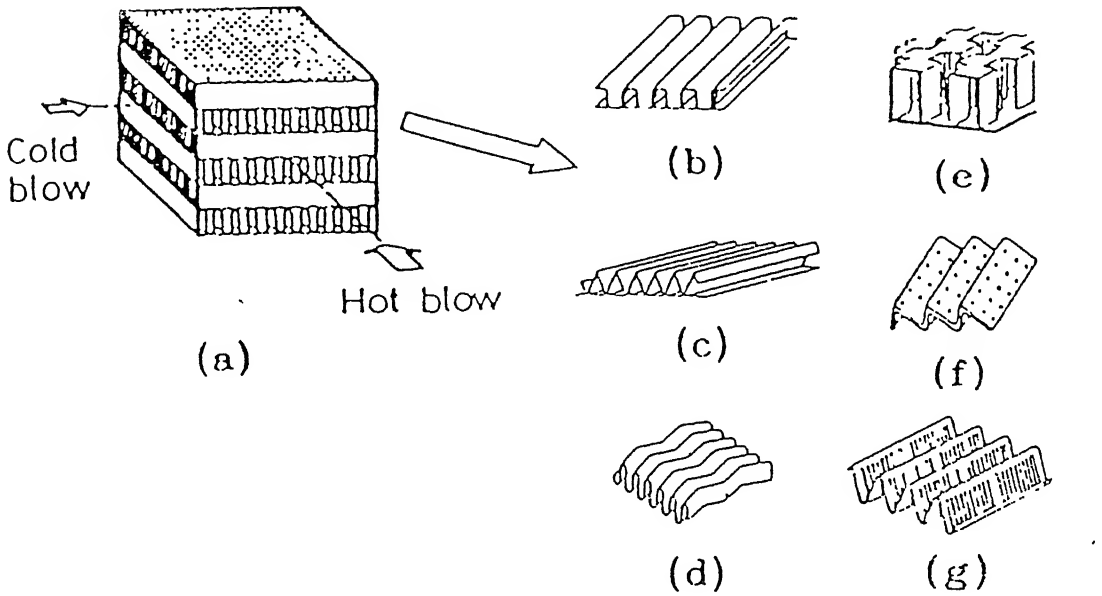

Figure 2.3 : (a)Plate –fin heat exchanger and its surface geometries: (b) plain rectangular fins (c) plain triangular fins (d)wavy fins (e) offset strip (f) perforated fins (g)louvered fins; after Webb (1987)

by using a multi-louvered surface geometry for the plates. Investigations by Achaichia and Cowell (1988) provide a detailed performance data for louvered fin surfaces. However in using louvered fins, enhancement is obtained at the price of high-pressure drop. To circumvent this difficulty, protrusions in the form of slender delta wings or winglets can be deployed (Fig.2.3). As shown, the base of the wing remains attached to the fin and the apex faces the incoming stream with an angle of attack with this configuration. The longitudinal vortices are generated along the side edge of the wing-shaped vortex generator due to the pressure difference between the front surface facing the flow and the back surface (Fig.2.3). These longitudinal vortices, generated by the vortex generators, can be made to disrupt the growth of boundary layer in a channel by

exchanging the fluid from the near-wall-region with the channel-core-region and thus they can serve to enhance the heat transfer rate while producing less of a pressure drop. Use of longitudinal vortices for boundary layer control is well known (Pearcey, 1961) and the vortex generators are used in commercial airplanes for this purpose.

MAC algorithm which is described below, calculates the velocitiy in U, V and W directions as well as it calculates the pressure P and temperature θ. These values are used by post-processing computer code (written separately), for the final calculation of Nusselt number, Apparent friction factor etc.

2.2 Problem Formulation

2.2.1 Introduction to the MAC (Marker and Cell) Method

The important ideas on which the MAC algorithm is based are:

1. Unsteady Navier-Stokes equations for incompressible flow in weak conservative form and the continuity equation are the governing equations.
2. Description of the problem is elliptic in space and parabolic in time. Solution will be marched in the time direction. At each time step, a converged solution in space domain is obtained but this converged solution at any time step may not be the solution of the physical problem.
3. If the problem is steady, in its physical sense, then after a finite number of steps in time direction, two consecutive time steps will show identical solutions. However in a machine-computation this is not possible hence very small value say, 'STAT' is predefined. Typically, STAT may be chosen between 10^{-3} and 10^{-5}. If the maximum discrepancy of any of the velocity components for two consecutive time steps at any location over the entire space does not exceed 'STAT' then it can be said that the steady solution has been evolved.
4. If the physical problem is basically unsteady in nature, the aforesaid maximum discrepancy of any dependent variable for two consecutive time steps will never be less than 'STAT'. However, for such a situation, a velocity component can be stored over a long duration of time and plot of the velocity component against time depicts the character of flow. Such a flow may be labeled as simply 'unsteady'.

5. With the help of momentum equations, we compute explicitly a provisional value of the velocity components for the next time step.

Consider the weak conservative form of non-dimensional momentum equation in the X direction:

$$\frac{\partial u}{\partial t}+\frac{\partial(u^2)}{\partial x}+\frac{\partial(uv)}{\partial y}+\frac{\partial(uw)}{\partial z}=-\frac{\partial p}{\partial x}+\frac{1}{\mathrm{Re}}\nabla^2 u$$

It is assumed that at t =nth level, we have a converged solution. Then for the next time step

$$\frac{u_{i,j,k}^{n+1}-u_{i,j,k}^{n}}{\Delta t}=[RESIDU]_{i,j,k}^{n}$$

or,

$$u_{i,j,k}^{n+1}=u_{i\,j\,k}^{n}+\Delta t[RESIDU]_{i,j,k}^{n}$$

$[RESIDU]_{i,j,k}^{n}$ consists of convective and diffusive terms, and the pressure gradient. Similarly, the provisional values for $v_{i,j,k}^{n+1}$ and $w_{i,j,k}^{n+1}$ can be explicitly computed. These explicitly advanced velocity components may not constitute a realistic flow field. A divergence free velocity field has to exist in order to describe a plausible incompressible flow situation. Now, with these provisional $u_{i,j,k}^{n+1}, v_{i,j,k}^{n+1}$ and $w_{i,j,k}^{n+1}$ values, continuity equation is evaluated in each cell. If $\nabla .V$ produces a nonzero value, there must be some amount of mass accumulation or annihilation in each cell, which is not physically possible, leading to an incorrect pressure field. Therefore, pressure at any cell is directly linked with the value of $(\nabla .V)$ at the cell. Now, on one hand the pressure has to be corrected with the help of non-zero divergence value and on the other, the velocity components have to be adjusted. The correction procedure continues through an iterative cycle till the divergence free velocity field is ensured.

Boundary conditions are to be applied after each explicit evaluation for the time step is accomplished. Since the governing equations are elliptic in space, boundary conditions on all confirming surfaces are required. Moreover, the boundary conditions are also to be applied after every pressure velocity iteration. The five principal kinds of boundary conditions to be considered are rigid no-slip walls, free-slip walls, in flow and outflow boundaries, and periodic (repeating) boundaries. (Biswas, G., (1995), Solution of Navier-

Stokes Equations for Incompressible Flows Using MAC and SIMPLE Algorithms, in *Computational Fluid Flow and Heat Transfer,* ed. K. Muralidhar and T. Sundararajan, Narosa Publishing House, India.)

2.2.2 Governing Equations for Laminar Flow

The dimensionless equations for continuity, momentum and energy for laminar incompressible flow may be expressed in their conservative forms as following:

$$D \equiv \frac{\partial U}{\partial X} + \frac{\partial V}{\partial Y} + \frac{\partial W}{\partial Z} = 0 \tag{2.1}$$

$$\frac{\partial U}{\partial \tau} + \frac{\partial U^2}{\partial X} + \frac{\partial UV}{\partial Y} + \frac{\partial UW}{\partial Z} = -\frac{\partial P}{\partial X} + \frac{\nabla^2 U}{\mathrm{Re}} \tag{2.2}$$

$$\frac{\partial V}{\partial \tau} + \frac{\partial UV}{\partial X} + \frac{\partial V^2}{\partial Y} + \frac{\partial VW}{\partial Z} = -\frac{\partial P}{\partial Y} + \frac{\nabla^2 V}{\mathrm{Re}} \tag{2.3}$$

$$\frac{\partial W}{\partial \tau} + \frac{\partial UW}{\partial X} + \frac{\partial VW}{\partial Y} + \frac{\partial W^2}{\partial Z} = -\frac{\partial P}{\partial Z} + \frac{\nabla^2 W}{\mathrm{Re}} \tag{2.4}$$

$$\frac{\partial \theta}{\partial \tau} + \frac{\partial U\theta}{\partial X} + \frac{\partial V\theta}{\partial Y} + \frac{\partial W\theta}{\partial Z} = \frac{\nabla^2 \theta}{\mathrm{Re.Pr}} \tag{2.5}$$

In the above equations, velocities have been non-dimensionalized with the average incoming velocity U_{av} at the channel inlet, all lengths with the channel height H, the pressure with ρU_{av}^2 and the non-dimensional temperature is defined as, $\theta = (T-T_\infty)/(T_w-T_\infty)$. The Reynolds number and the Prandtl number are defined by Re and Pr respectively.

2.2.3 Boundary Conditions for Laminar Flow

The boundary conditions of interest in this investigation are (refer Fig. 2.4):

- Top and bottom plates:

$$U = V = W = 0; \quad \theta = 1 \tag{2.6}$$

- Side wall ($z = B/2$) and midplane ($z = 0$):

$$W = (\frac{\partial V}{\partial Z}) = (\frac{\partial U}{\partial Z}) = 0; (\frac{\partial \theta}{\partial Z}) = 0 \qquad (2.7)$$

- At the channel inlet:

$$U = U(Y),\ V=W=0;\ \theta = 0 \qquad (2.8)$$

- At the exit; a smooth transition through the outflow boundary is ensured by setting:

$$\frac{\partial^2 U}{\partial X^2} = \frac{\partial^2 V}{\partial X^2} = \frac{\partial^2 W}{\partial X^2} = 0; \frac{\partial^2 \theta}{\partial X^2} = 0 \qquad (2.9)$$

No-slip boundary conditions for the velocities on the obstacles are used. The temperature of the obstacle is considered constant and equal to T_w.

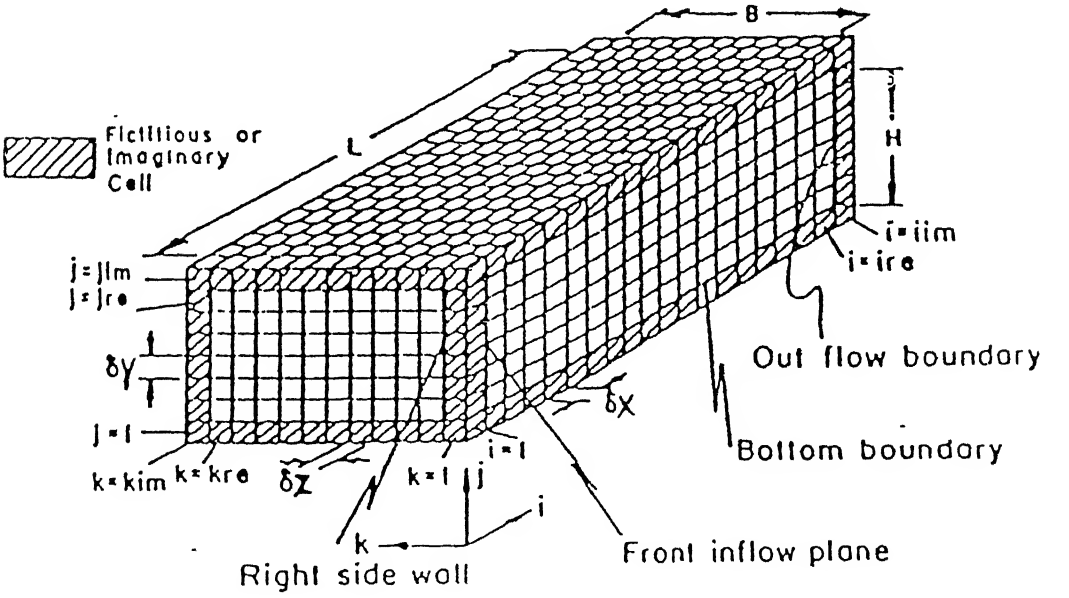

Figure2.4: Boundary conditions and fictitious boundary cells

2.2.4 Grid System Used

Computational domain is divided into a set of rectangular cells (Fig.2.5(a)) and a staggered grid arrangement is used such that velocity components are defined at the center of the cell faces to which they are normal (Fig2.5 (b)). The pressure and temperature are defined at the center of the cell. In such an arrangement, pressure difference between two adjacent cells. The pressure field will accept a reasonable pressure distribution for a correct velocity field. Another important advantage of such a grid system is that transport rates across the faces of the control volumes can be computed without interpolation of velocity components.

2.2.5 Boundary Conditions for Confining Walls

Since, the equations are elliptic in space, we need boundary conditions on all confining walls, -even at the outlet. Consider, for example, the bottom boundary of the computing (physical) mesh. If this boundary is to be a rigid no-slip wall, the normal velocity on the wall must be zero. Here, we are considering a stationary wall. With reference to Fig.2.5 (b), we have

$$\left.\begin{aligned} V_{i,1,k} &= 0 \\ U_{i,1,k} &= -U_{i,2,k} \\ W_{i,1,k} &= -W_{i,2,k} \end{aligned}\right\} \quad \begin{aligned} &\text{For i = 2 to ire} \\ &\text{And k = 2 to kre} \end{aligned} \qquad (2.10)$$

If the right side wall is a free-slip (vanishing shear) boundary, the normal velocity must be zero and the tangential velocities should have no normal gradient.

$$\left.\begin{aligned} W_{i,J,1} &= 0 \\ U_{i,J,1} &= -U_{i,J,2} \\ V_{i,J,1} &= -V_{i,J,2} \end{aligned}\right\} \quad \begin{aligned} &\text{For i = 2 to ire} \\ &\text{And j = 2 to jre} \end{aligned} \qquad (2.11)$$

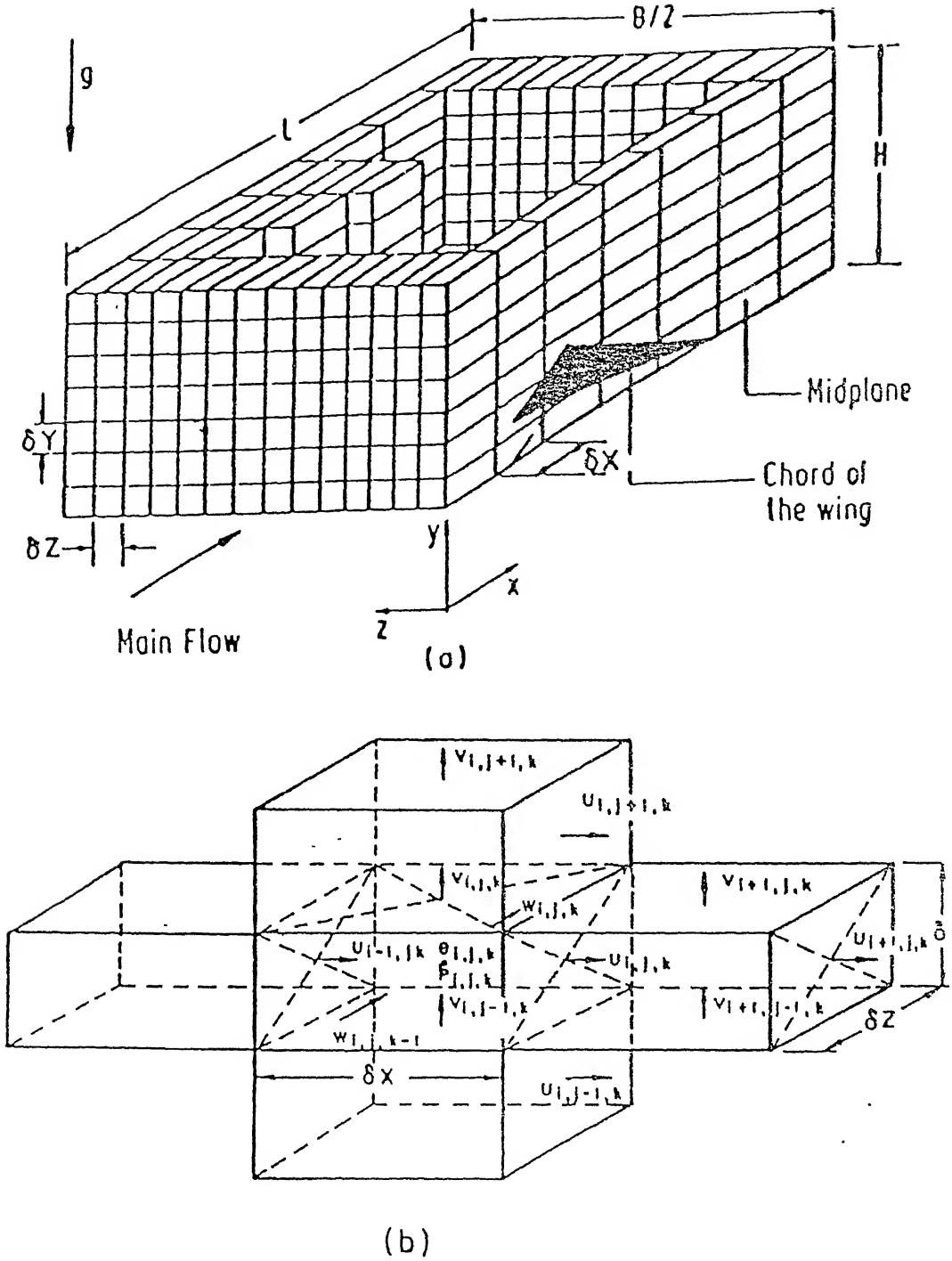

Figure 2.5 (a) Grid spacing in the computational domain and the location of the wing type vortex grid showing the descretized variables (b) Three dimensional staggered grid showing the locations of the descretized variables.

The front plane is to be provided with inflow boundary condition. Any desired functional relationship may be recommended. Generally, normal velocity components are set to zero and a uniform or parabolic axial velocity may be deployed. Hence, with reference to Fig. (2.5(b)), we can write

$$\left.\begin{aligned} V_{1,J,k} &= -V_{2,J,k} \\ W_{1,J,k} &= -W_{2,J,k} \\ U_{1,J,k} &= 1.0 \\ or, U_{1,J,k} &= 1.5*[1-(\frac{j_m - j}{j_m})^2] \end{aligned}\right\} \quad \begin{aligned} &\text{For j = 2 to ire} \\ &\text{And k = 2 to kre} \end{aligned} \qquad (2.12)$$

where, j_m is the horizontal midplane.

Continuative or outflow boundaries always pose a problem for low-speed calculations, because whatever prescription is chosen it can affect the entire flow field upstream. What is needed is a prescription that permits fluid to flow out of the mesh with a minimum of upstream influence. In MAC family of algorithms, the second derivatives of the dependent variables in flow direction are set to zero in order to ensure smooth transition through the outflow boundary. These are implemented in the following way:

$$\left.\begin{aligned} U_{i+1,J,k} &= 2U_{i,j,k} - U_{i-1,J,k} \\ V_{i+1,J,k} &= 2V_{i,j,k} - V_{i-1,J,k} \\ W_{i+1,J,k} &= 2W_{i,J,k} - W_{i-1,j,k} \end{aligned}\right\} \quad \begin{aligned} &For\ j = 2\ to\ jre \\ &And\ k = 2\ to\ kre \\ &At\quad i = iim - 2 \end{aligned} \qquad (2.13)$$

2.2.6 Boundary Conditions for the Obstacle

A special effort is required to satisfy the kinematic boundary conditions on the vortex generator. From Fig. (2.6), the angle of attack of the wing-type vortex generator can be expressed as $\beta = \tan^{-1}(\delta Y / \delta X)$. Fig. (2.6) further reveals that the U and V components of velocity fall directly on the surface of the obstacle in the region of the wing and are therefore equal to zero. Implementation of no-slip condition for U component velocity at

the side edge of the obstacle needs some manipulations. From Fig.(2.6), it is found that $U_{i,j,k+1/2} = 0$. In the other words, we can write

$$U_{i,j,k} = -U_{i,j,k+1}$$

(for i=ia to ib, j =2 to ja and k = 2 to kc) (2.14)

It may be mentioned that the difference of count between kc and 2 is equal to that between ib and ia. The W component of velocity also needs manipulation for its zero value on the surface of the obstacle. From Fig.(2.7)

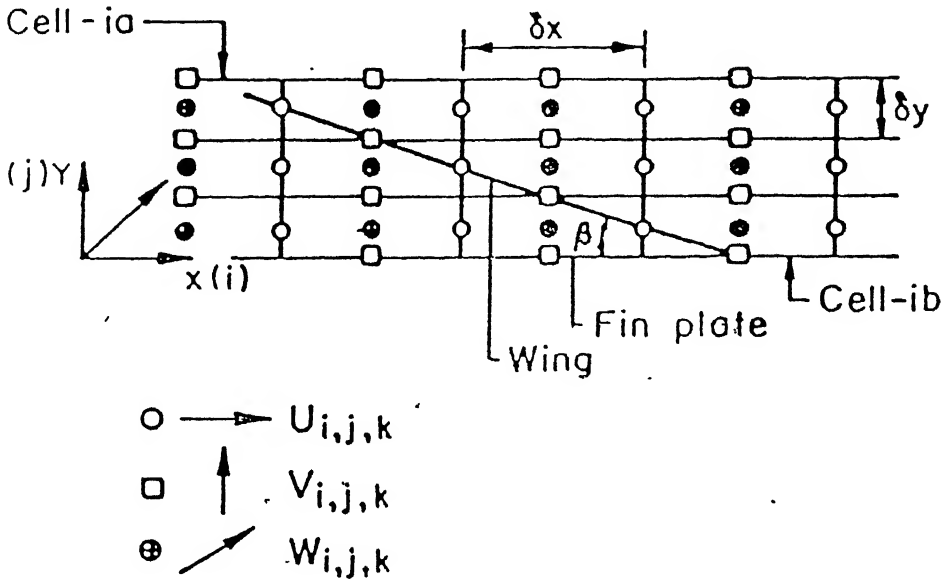

Figure 2 6: Relative location of velocity components and wing on X-Y plane at Z=0

$$\left.\begin{aligned} W_{i,j,k} &= -W_{i,j-1,k} \\ W_{i,j,k} &= -W_{i-1,j,k} \\ W_{i,j-1,k} &= -W_{i,j,k} \\ W_{i-1,j,k} &= W_{i,j,k} \end{aligned}\right\} \quad (2.15)$$

(for i = ia to ib, j =2 to ja and k =2 to kc)

The temperature boundary conditions on the wing-type obstacle are diagrammatically shown in Fig.(2.8). The obstacle boundary conditions for temperature are:

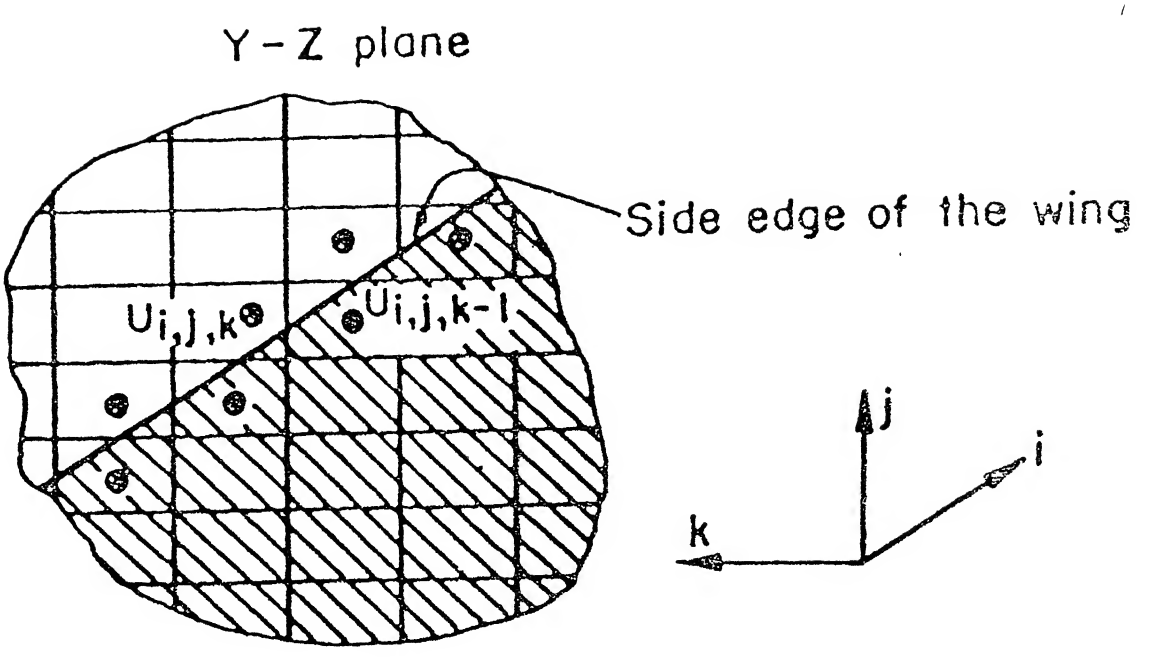

Figure 2.7: Side edge of the wing-type vortex generator on Y-Z plane.

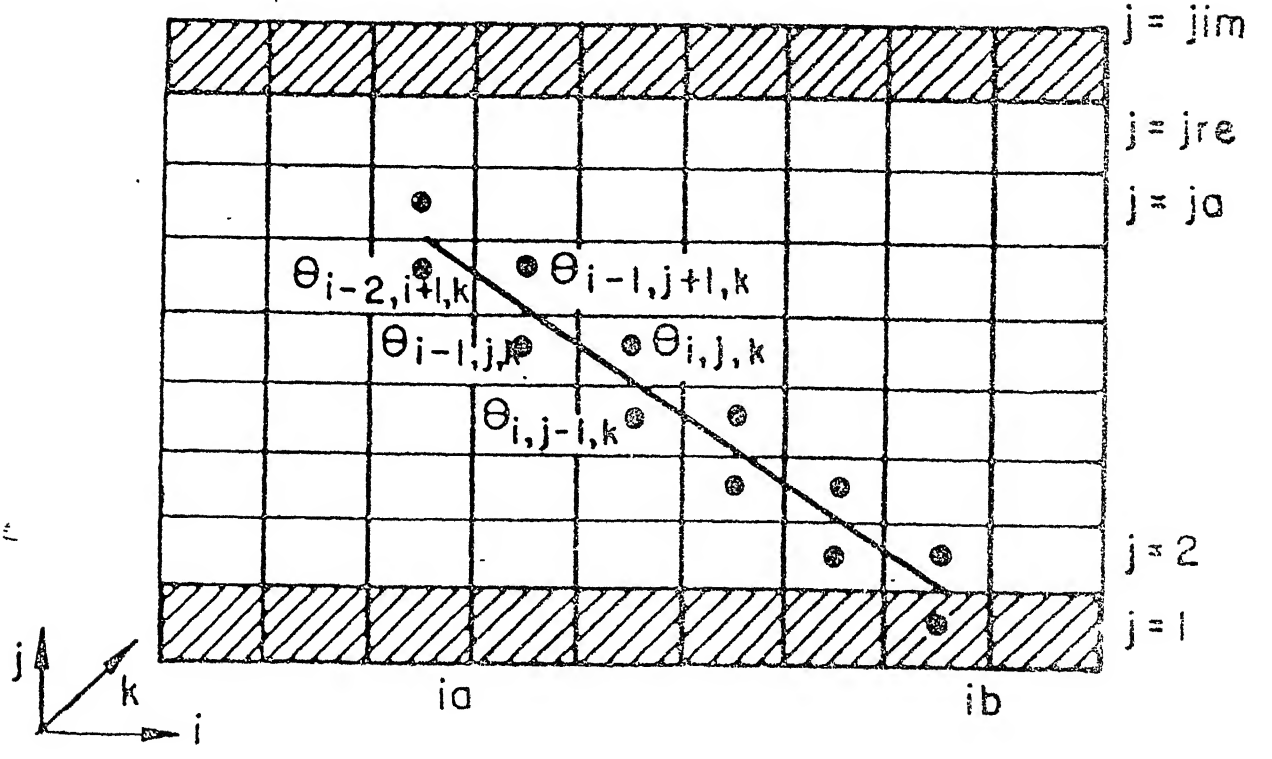

Figure 2.8: Thermal boundary conditions on the wing-type vortex

$$\left.\begin{aligned}
\theta_{i,j,k} &= 2\theta_w - \theta_{i-1,j,k} \\
\theta_{i,j,k} &= 2\theta_w - \theta_{i,j-1,k} \\
\theta_{i-1,j+1,k} &= 2\theta_w - \theta_{i-1,j,k} \\
\theta_{i-1,j+1,k} &= 2\theta_w - \theta_{i-2,j+1,k}
\end{aligned}\right\} \qquad (2.16)$$

(for i =ia to ib, j = 2 to ja and k =2 to kc)

In practice, the vortex generators can easily be manufactured by punching or embossing the wall. In some computational results, the effects due to the hole beneath the vortex generator have been taken into account. It is considered that the heat exchanger cores

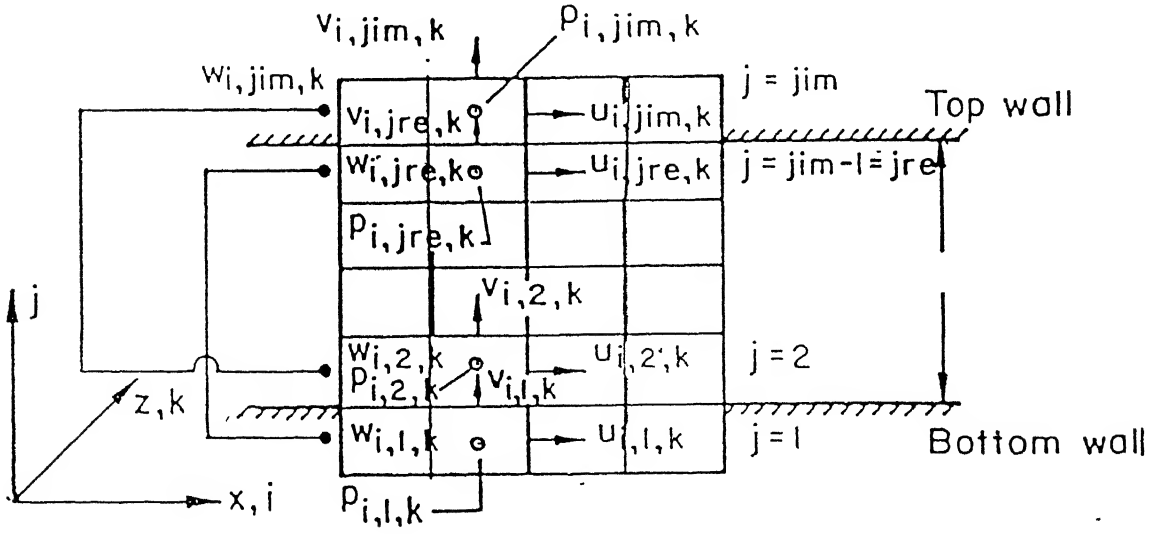

Figure 2.9 : Periodic boundary conditions for pressure and velocities on the top and the bottom wall.

have a number of plates and on each plate the vortex generators are punched out in such a way that the holes are perfectly aligned. In our computational domain, a small part of top and bottom boundaries must be set to identify the punched holes. For this purpose spacewise-periodic boundary conditions on the location of the punched holes have to be applied in the y-direction (Fig.2.9). Here, the period length is channel height 'H'. However boundary conditions for the fictitious cells on the bottom are:

$$\left.\begin{aligned} U_{i,1,k} &= U_{i,jre,k} \\ V_{i,1,k} &= 0.5(V_{i,jre,k} + V_{i,1,k}) \\ W_{i,1,k} &= W_{i,jre,k} \\ P_{i,1,k} &= P_{i,jre,k} \end{aligned}\right\} \qquad (2.17)$$

(for all i, k in the punched holes)

and on the top

$$\left.\begin{aligned} U_{i,jim,k} &= U_{i,2,k} \\ V_{i,jim,k} &= V_{i,2,k} \\ V_{i,jre,k} &= 0.5(V_{i,jre,k} + V_{i,1,k}) \\ W_{i,jim,k} &= W_{i,2,k} \\ P_{i,jim,k} &= P_{i,2,k} \end{aligned}\right\} \qquad (2.18)$$

(for all i,k in the punched holes)

Such boundary conditions have also been discussed by Hirt et al. (1975) and Biswas and Chattopadhyay (1992). However, for plate-fin heat exchangers, a different manufacturing technique for mounting the vortex generators is adapted. For this case, no hale exists underneath the vortex generators in order to avoid mixing of the hot and cold streams.

2.3 MAC (Marker and Cell) Algorithm

Because of staggered grid arrangement (Fig.2.5), the velocities are not defined at the nodal points. Whenever required, the velocities at the nodal points are to be found by interpolation. For example, with uniform grids, we can write $U_{i-\frac{1}{2},j,k} = 0.5(U_{i-1,j,k}+U_{i,j,k})$. Where a product or square of such quantity appears, it is to be averaged first and then the product is to be formed.

Convective terms of the momentum equations are discretized using a weighted average of second upwind and space centered scheme (Hirt et al., 1975). Diffusive terms are discretized by a central difference scheme. Let us consider the discretized terms of x-momentum equation (refer to Fig. *).

$$\left[\frac{\partial U^2}{\partial X}\right]_{i,j,k} = \frac{1}{4\delta X}\begin{bmatrix}(U_{i,j,k}+U_{i+1,j,k})(U_{i,j,k}+U_{i+1,j,k})+\alpha_p\,|(U_{i,j,k}+U_{i+1,j,k})|(U_{i,j,k}-U_{i+1,j,k})\\-(U_{i-1,j,k}+U_{i,j,k})(U_{i-1,j,k}+U_{i,j,k})-\alpha_p\,|(U_{i-1,j,k}+U_{i,j,k})|(U_{i-1,j,k}-U_{i,j,k})\end{bmatrix}$$

$$\equiv \text{DUUDX} \qquad (2.19)$$

$$\left[\frac{\partial UV}{\partial X}\right]_{i,j,k} = \frac{1}{4\delta Y}\begin{bmatrix}(V_{i,j,k}+V_{i+1,j,k})(U_{i,j,k}+U_{i,j+1,k})+\alpha_p\,|(V_{i,j,k}+V_{i+1,j,k})|(U_{i,j,k}-U_{i,j+1,k})\\-(V_{i,j-1,k}+V_{i+1,j-1,k})(U_{i,j-1,k}+U_{i,j,k})-\alpha_p\,|(V_{i,j-1,k}+V_{i+1,j-1,k})|(U_{i,j-1,k}-U_{i,j,k})\end{bmatrix}$$

$$\equiv \text{DUVDY} \qquad (2.20)$$

$$\left[\frac{\partial UW}{\partial Z}\right]_{i,j,k} = \frac{1}{4\delta Z}\begin{bmatrix}(W_{i,j,k}+W_{i+1,j,k})(U_{i,j,k}+U_{i,j,k+1})+\alpha_p\,|(W_{i,j,k}+W_{i+1,j,k})|(U_{i,j,k}-U_{i,j,k+1})\\-(W_{i,j,k-1}+W_{i+1,j,k-1})(U_{i,j,k-1}+U_{i,j,k})-\alpha_p\,|(W_{i,j,k-1}+W_{i+1,j,k-1})|(U_{i,j,k-1}-U_{i,j,k})\end{bmatrix}$$

$$\equiv \text{DUWDZ} \qquad (2.21)$$

$$\frac{\partial P}{\partial X} = \frac{P_{i+1,j,k}-P_{i,j,k}}{\delta X} \equiv DPDX \qquad (2.22)$$

$$\frac{\partial^2 U}{\partial X^2} = \frac{U_{i+1,j,k}-2U_{i,j,k}+U_{i-1,j,k}}{(\delta X^2)} \equiv D2UDX2 \qquad (2.23)$$

with, $\alpha_p \longrightarrow 1$, the scheme tends to second upwind and $\alpha_p \longrightarrow 0$, the scheme tends to Space centered.

The factor α_p is chosen in such a way that the differencing scheme retains 'something' of second order accuracy and the required upwinding is done for the sake of stability. A typical value of α_p is between 0.2. and 0.3.

Solutions for the velocities are obtained in two folds. First, the velocity components are advanced explicitly using the previous state of the flow, having calculated accelerations caused by convection, diffusion and pressure gradients through a time step $\delta\tau$. The explicit time increment may not necessarily lead to a velocity field with zero mass divergence in each cell. In the subsequent fold, adjustment of pressure and velocity is done by an iterative process in order to ensure mass conservation in each cell. If the explicitly advanced provisional velocity is termed as $\tilde{U}^{n+1}_{i,J,k}$, then from equation (*) we can write

$$\tilde{U}^{n+1}_{i,J,k} = U^{n}_{i,J,k} + \delta\tau\left[RESIDU\right]^{n}_{i,J,k} \tag{2.24}$$

where,

$$\left[RESIDU\right]^{n}_{i,J,k} = \begin{bmatrix} (-DUUDX - DUVDY - DUWDZ) - DPDX \\ +(1/\mathrm{Re})(D2UDX2 + D2UDY2 + D2UDZ2) \end{bmatrix} \tag{2.25}$$

In a similar manner we evaluate

$$\tilde{V}^{n+1}_{i,J,k} = V^{n}_{i,J,k} + \delta\tau\left[RESIDV\right]^{n}_{i,J,k} \tag{2.26}$$

$$\tilde{W}^{n+1}_{i,J,k} = W^{n}_{i,J,k} + \delta\tau\left[RESIDW\right]^{n}_{i,J,k} \tag{2.27}$$

As discussed earlier, the explicitly advanced tilde velocities may not necessarily lead to a flow field with zero mass divergence in each cell. This implies that at this stage the pressure distribution is not correct. Pressure in each cell will be corrected in such a way that there is no net mass flow in or out of the cell. In the original MAC metohd, the corrected pressures are obtained from the solution of a Poisson equation for pressure. A related technique developed by Chorin (1967) involved a simultaneous iteration on

pressures and velocity components. Vicelli (1971) has shown that the two methods as applied to the MAC method are equivalent. We shall make use of the iterative correction procedure of Chorin (1967) in order to obtain a divergence-free velocity field. The mathematical methodology of this iterative pressure-velocity correction procedure will be discussed herein.

The relationship between the explicitly advanced velocity component and the velocity at the previous time step may be written as

$$\tilde{U}^{n+1}_{i,J,k} = U^{n}_{i,J,k} + \frac{\delta\tau\left[P^{n}_{i,J,k} + P^{n}_{i+1,J,k}\right]}{\delta X} + \delta\tau\left[CONDIFU\right]^{n}_{i,J,k} \tag{2.28}$$

$$\left[CONDIFU\right]^{n}_{i,J,k} = \left[RESIDU\right]^{n}_{i,J,k} + \left[DPDX\ \right]^{n}_{i,J,k} \tag{2.29}$$

where, on the other hand, the corrected velocity-component (unknown) will be related to the correct pressure (also known) in the following way:

$$U^{n+1}_{i,J,k} = U^{n}_{i,J,k} + \frac{\delta\tau\left[P^{n+1}_{i,J,k} - P^{n+1}_{i+1,J,k}\right]}{\delta X} + \delta\tau\left[CONDIFU\right]^{n}_{i,J,k} \tag{2.30}$$

from equations (*) & (*) we can write

$$U^{n+1}_{i,J,k} - \tilde{U}^{n+1}_{i,J,k} = \frac{\delta\tau\left[P'_{i,J,k} - P'_{i+1,J,k}\right]}{\delta X} \tag{2.31}$$

where the pressure is defined as

$$P'_{i,J,k} = P^{n+1}_{i,J,k} - P^{n}_{i,J,k} \tag{2.32}$$

Neither the pressure corrections nor $U^{n+1}_{i,J,k}$ are known explicitly at this stage so one can not be calculated with the help of the other. Calculations are done in an iterative cycle and we write

$$U^{n+1}_{i,J,k} = \tilde{U}^{n+1}_{i,J,k} + \frac{\delta\tau\left[P'_{i,J,k} - P'_{i+1,J,k}\right]}{\delta X}$$

In a similar way, we can formulate the following array:

Corrected Estimated Correction

$$U^{n+1}_{i,J,k} \quad \rightarrow \quad \tilde{U}^{n+1}_{i,J,k} \quad + \quad \frac{\delta\tau\left[P'_{i,J,k} - P'_{i+1,J,k}\right]}{\delta X} \tag{2.33}$$

$$U_{i-1,j,k}^{n+1} \rightarrow \tilde{U}_{i-1,j,k}^{n+1} - \frac{\delta\tau\left[P'_{i,j,k} - P'_{i-1,j,k}\right]}{\delta X} \tag{2.34}$$

$$V_{i-1,j,k}^{n+1} \rightarrow \tilde{V}_{i,j,k}^{n+1} + \frac{\delta\tau\left[P'_{i,j,k} - P'_{i,j+1,k}\right]}{\delta Y} \tag{2.35}$$

$$V_{i,j,k}^{n+1} \rightarrow \tilde{V}_{i,j-1,k}^{n+1} - \frac{\delta\tau\left[P'_{i,j,k} - P'_{i,j-1,k}\right]}{\delta Y} \tag{2.36}$$

$$W_{i,j,k}^{n+1} \rightarrow \tilde{W}_{i,j,k}^{n+1} + \frac{\delta\tau\left[P'_{i,j,k} - P'_{i,j,k+1}\right]}{\delta Z} \tag{2.37}$$

$$W_{i-1,j,k}^{n+1} \rightarrow \tilde{W}_{i,j,k-1}^{n+1} - \frac{\delta\tau\left[P'_{i,j,k} - P'_{i,j,k-1}\right]}{\delta Z} \tag{2.38}$$

The correction is done through continuity equation. Plugging-in the above relationship into the continuity equation (*) we shall obtain

$$\left[\frac{U_{i,j,k}^{n+1} - U_{i-1,j,k}^{n+1}}{\delta X} + \frac{V_{i,j,k}^{n+1} - V_{i,j-1,k}^{n+1}}{\delta Y} + \frac{W_{i,j,k}^{n+1} - W_{i,j,k-1}^{n+1}}{\delta Z}\right]$$

$$= \left[\frac{\tilde{U}_{i,j,k}^{n+1} - \tilde{U}_{i-1,j,k}^{n+1}}{\delta X} + \frac{\tilde{V}_{i,j,k}^{n+1} - \tilde{V}_{i,j-1,k}^{n+1}}{\delta Y} + \frac{\tilde{W}_{i,j,k}^{n+1} - \tilde{W}_{i,j,k-1}^{n+1}}{\delta Z}\right]$$

$$-\delta\tau\left[\frac{P'_{i+1,j,k} - 2P'_{i,j,k} + P'_{i-1,j,k}}{(\delta X^2)} + \frac{P'_{i,j+1,k} - 2P'_{i,j,k} + P'_{i,j-1,k}}{(\delta Y^2)} + \frac{P'_{i,j,k+1} - 2P'_{i,j,k} + P'_{i,j,k-1}}{(\delta Z^2)}\right] \tag{2.39}$$

or,

$$\left[\frac{U_{i,j,k}^{n+1} - U_{i-1,j,k}^{n+1}}{\delta X} + \frac{V_{i,j,k}^{n+1} - V_{i,j-1,k}^{n+1}}{\delta Y} + \frac{W_{i,j,k}^{n+1} - W_{i,j,k-1}^{n+1}}{\delta Z}\right]$$

$$= \left[\frac{\tilde{U}_{i,j,k}^{n+1} - \tilde{U}_{i-1,j,k}^{n+1}}{\delta X} + \frac{\tilde{V}_{i,j,k}^{n+1} - \tilde{V}_{i,j-1,k}^{n+1}}{\delta Y} + \frac{\tilde{W}_{i,j,k}^{n+1} - \tilde{W}_{i,j,k-1}^{n+1}}{\delta Z}\right]$$

$$+\left[\frac{2\delta\tau(P'_{i,J,k})}{\delta X^2}+\frac{2\delta\tau(P'_{i,J,k})}{\delta Y^2}+\frac{2\delta\tau(P'_{i,J,k})}{\delta Z^2}\right] \tag{2.40}$$

In deriving the above expression, it is assumed that the pressure corrections in the neighboring cells are zero. Back to the calculations, we can write

$$0=(D)_{i,J,k}+P'_{i,J,k}\left[2\delta\tau(\frac{1}{\delta X^2}+\frac{1}{\delta Y^2}+\frac{1}{\delta Z^2}\right] \tag{2.41}$$

or,
$$P'_{i,J,k}=\frac{-(D)_{i,J,k}}{\left[2\delta\tau(\frac{1}{\delta X^2}+\frac{1}{\delta Y^2}+\frac{1}{\delta Z^2}\right]} \tag{2.42}$$

In order to accelerate the calculation, the pressure correction equation is modified as

$$P'_{i,J,k}=\frac{-\omega_0(D)_{i,j,k}}{\left[2\delta\tau(\frac{1}{\delta X^2}+\frac{1}{\delta Y^2}+\frac{1}{\delta Z^2}\right]} \tag{2.43}$$

where ω_0 is the overrelaxation factor. A value of $\omega_0 = 1.7$ is commonly used. After calculating $P'_{i,J,k}$ the pressure in the cell (i,j,k) is adjusted as

$$P^{n+1}_{i,J,k}\rightarrow P^{n}_{i,J,k}+P'_{i,J,k} \tag{2.44}$$

Now the pressure and velocity components for each cell are corrected through an iterative procedure in such a way that for the final pressure field, the velocity divergence in each cell vanishes. The process is continued till divergence-free velocity field is reached with a prescribed upper bound; here a value of 0.0001 is recommended. This solution scheme is continued until a steady flow is obtained.

Finally we discuss another important observation. If the velocity boundary conditions are correct pressure will be determined in all the cells including the cells at the boundary. Thus, this method avoids the application of pressure boundary conditions. This typical feature of modified MAC method has been discussed in more details by Peyret and Taylor(1983).

Discretization Technique for k and ε Equations:

Convective terms of k and ε equations are also discretized using a weighted average of second upwind and space centered scheme (Hirt et al., 1975). Diffusive terms are discretized by a central difference scheme.

Let us consider the discretized terms of the k equation

$$\left[\frac{\partial kU}{\partial X}\right]_{i,j,k} = \frac{1}{2\delta X}\begin{bmatrix}(k_{i,j,k}+k_{i+1,j,k})U_{i,j,k}+\alpha_p(k_{i,j,k}-k_{i+1,j,k})\,|U_{i,j,k}| \\ -(k_{i-1,j,k}+k_{i,j,k})U_{i-1,j,k}-\alpha_p\,|U_{i-1,j,k}|\,(k_{i-1,j,k}-k_{i,j,k})\end{bmatrix}$$

$$\equiv DkUDX \tag{2.45}$$

$$\left[\frac{\partial}{\partial X}(\nu_t\frac{\partial k}{\partial X})\right]_{i,j,k} = \frac{1}{2(\delta X^2)}\begin{bmatrix}((\nu_t)_{i,j,k}+(\nu_t)_{i+1,j,k})(k_{i-1,j,k}-k_{i,j,k})- \\ ((\nu_t)_{i-1,j,k}+(\nu_t)_{i,j,k})(k_{i,j,k}-k_{i-1,j,k})\end{bmatrix}$$

$$\equiv \text{DIFFkX} \tag{2.46}$$

The difference quotients involved in the Generation term are discretized as following.

$$\frac{\partial U}{\partial X} = \frac{U_{i,j,k}-U_{i-1,j,k}}{\delta X} \equiv DUDX \tag{2.47}$$

$$\frac{\partial V}{\partial Y} = \frac{V_{i,j,k}-V_{i,j-1,k}}{\delta Y} \equiv DVDY \tag{2.48}$$

$$\frac{\partial W}{\partial Z} = \frac{W_{i,j,k}-W_{i,j,k-1}}{\delta Z} \equiv DWDZ \tag{2.49}$$

$$\frac{\partial U}{\partial Y} = \frac{1}{4\delta Y}\left[(U_{i,j,k}+U_{i-1,j,k}+U_{i,j+1,k}+U_{i-1,j+1,k})-(U_{i,j,k}+U_{i-1,j,k}+U_{i,j-1,k}+U_{i-1,j-1,k})\right]$$

$$\equiv \text{DUDY} \tag{2.50}$$

$$\frac{\partial V}{\partial X} = \frac{1}{4\delta X}\left[(V_{i,j,k}+V_{i,j-1,k}+V_{i+1,j,k}+V_{i+1,j-1,k})-(V_{i,j,k}+V_{i,j-1,k}+V_{i-1,j,k}+V_{i-1,j-1,k})\right]$$

$$\equiv \text{DVDX} \tag{2.51}$$

$$\frac{\partial W}{\partial X} = \frac{1}{4\delta X}\left[(W_{\iota,J,k} + W_{\iota,J,k-1} + W_{\iota+1,J,k} + W_{\iota+1,J,k-1}) - (W_{\iota,J,k} + W_{\iota,J,k-1} + W_{\iota-1,j,k} + W_{\iota-1,J,k-1})\right]$$

$$\equiv \text{DWDX} \tag{2.52}$$

$$\frac{\partial U}{\partial Z} = \frac{1}{4\delta Z}\left[(U_{\iota,J,k} + U_{\iota-1,J,k} + U_{\iota,J,k+1} + U_{\iota-1,j,k+1}) - (U_{i,j,k} + U_{\iota-1,J,k} + U_{\iota,J,k-1} + U_{\iota-1,J,k-1})\right]$$

$$\equiv \text{DUDZ} \tag{2.53}$$

$$\frac{\partial V}{\partial Z} = \frac{1}{4\delta Z}\left[(V_{\iota,J,k} + V_{\iota,J-1,k} + V_{\iota,J,k+1} + V_{\iota,J-1,k+1}) - (V_{\iota,J,k} + V_{\iota,J-1,k} + V_{\iota,J,k-1} + V_{\iota,J-1,k-1})\right]$$

$$\equiv \text{DVDZ} \tag{2.54}$$

$$\frac{\partial W}{\partial Y} = \frac{1}{4\delta X}\left[(W_{\iota,J,k} + W_{\iota,J,k-1} + W_{\iota,J+1,k} + W_{\iota,J+1,k-1}) - (W_{i,J,k} + W_{\iota,J,k-1} + W_{\iota,J-1,k} + W_{\iota,J-1,k-1})\right]$$

$$\equiv \text{DWDY} \tag{2.55}$$

In terms of the difference quotients, the ε equation consists of the similar quotients as the k equations.

Solutions of the Energy Equation:

After evaluating the correct velocities, the energy equation is solved with an successive Over-Relaxation technique to determine the temperature field. We shall discuss the solution procedure of the energy equation in this section.

The steady state energy equation, neglecting the dissipation term, may be written in the following conservative form as

$$\frac{\partial U\theta}{\partial X} + \frac{\partial V\theta}{\partial Y} + \frac{\partial W\theta}{\partial Z} = \frac{\nabla^2\theta}{Pe} \tag{2.56}$$

Equation (2.56) may be written as

$$\nabla^2\theta = Pe\left[CONVT\right]^m_{\iota,J,k} \tag{2.57}$$

where, $[CONVT]_{i,J,k}$ is the discretized convective terms on the left hand side of equation (2.56) and m stands for iterative counter. To start with, we can assume any guess value of θ throughout the flow field. U, V and W are known from the solution of momentum equation hence equation (2.57) is now linear equation. However, from the guess values of θ and known correct values of U, V and W the left hand side of equation (2.56) is evaluated. A weighted average scheme may be adapted for discretization of the convective terms. After discretizing and evaluating right hand side of equation (2.57) we obtain a Poisson equation for temperature with a source term on the right hand side. Now, we can follow a SOR technique for solving equation (2.57). Consider a discretized equation as

$$\frac{\theta_{i+1,J,k}-2\theta_{i,J,k}+\theta_{i-1,J,k}}{(\delta X)^2}+\frac{\theta_{i,J+1,k}-2\theta_{i,J,k}+\theta_{i,J-1,k}}{(\delta Y)^2}+\frac{\theta_{i,J,k+1}-2\theta_{i,j,k}+\theta_{i,J,k-1}}{(\delta Z)^2}=S^{*m}$$

where, $S^{*m} \equiv Pe[CONVT]^m_{i,J,k}$

or,

$$A^{*m}-\theta_{i,J,k}\left[\frac{2}{(\delta X)^2}+\frac{2}{(\delta Y)^2}+\frac{2}{(\delta Z)^2}\right]=S^{*m}$$

or, $$\theta_{i,J,k}=\frac{A^{*m}-S^{*m}}{\left[\frac{2}{(\delta X)^2}+\frac{2}{(\delta Y)^2}+\frac{2}{(\delta Z)^2}\right]} \qquad (2.58)$$

where,

$$A^{*m}=\frac{\theta_{i+1,J,k}+\theta_{i-1,J,k}}{(\delta X)^2}+\frac{\theta_{i,J+1,k}+\theta_{i,J-1,k}}{(\delta Y)^2}+\frac{\theta_{i,J,k+1}+\theta_{i,J,k-1}}{(\delta Z)^2}$$

$\theta_{i,J,k}$ in equation (*) may be assumed to be most recent value and it may be written as $\theta^{m'}_{i,J,k}$. In order to accelerate the speed of computation we introduce a over-relaxation factor ω and

$$\theta^{m+1}_{i,J,k}=\theta^{m}_{i,J,k}+\omega\left[\theta^{m'}_{i,J,k}-\theta^{m}_{i,J,k}\right] \qquad (2.59)$$

where $\theta^{m}_{i,j,k}$ is the previous value, $\theta^{m'}_{i,j,k}$ is the most recent value and $\theta^{m+1}_{i,j,k}$ is the calculated better guess. The procedure will continue till the required convergence is achieved.

Numerical Stability Considerations:

For accuracy, the mesh size must be chosen small enough to resolve the expected spatial variations in all dependent variables.

Once a mesh has been chosen, the choice of the time increment is governed by two restrictions, namely, the Courant-Friedrichs-Lewy (CFL) conditionand the restriction on the basis of grid-Fourier numbers.

According to the CFL condition, material cannot move through more than one cell in one time step. Therefore, the time increment must satisfy the inequality

$$\delta\tau < \min\left\{\frac{\delta X}{|U|}, \frac{\delta Y}{|V|}, \frac{\delta W}{|W|}\right\} \qquad (2.60)$$

where the minimum is with respect to every cell in the mesh. Typically, $\delta\tau$ is chosen equal to one-fourth to one-third of the minimum cell transit time. When the viscous diffusion terms are more important, the condition necessary to ensure stability is dictated by the restriction on the grid Fourier numbers, which results in

$$\delta\tau < \frac{1}{2}\frac{(\delta X)^2(\delta Y)^2(\delta Z)^2}{(\delta X^2 + \delta Y^2 + \delta Z^2)} \qquad (2.61)$$

The final $\delta\tau$ for each time increment is the minimum of the $\delta\tau$'s obtained from equations (2.60) and (2.61).

(This part of the thesis has been taken from Deb, Prashanta, (April, 1994), "*Three Dimensional Computation of Laminar and Turbulent Flows with Heat Transfer in a channel with Built-in Longitudinal Vortex Generators*", PhD. Thesis, ME Department, IIT Kanpur.)

2.4 Literature Survey

What originally motivated the introduction of EVOP, was the idea that the widespread and daily use of *simple* statistical design and analysis during r*outine* production by

process operatives themselves could reap enormous additional rewards. [Box and Draper (1969)]

An excellent review of industrial applications of EVOP has been presented by Hunter and Kittrell (1966). This review, which lists 68 references, discusses applications of EVOP in a wide variety of environments. Among these, applications in the chemical industry are most numerous, with special references to uses by the Dow Chemical Company [Anonymous (1961*a*, 1961*b*)], Imperial Chemical Industries Limited [Coutie (1959a, 1959b)], Tennessee Eastman Company [DeBusk (1962); Pursglove (1961); Wilson (1960)], the Chemstrand Corporation [Annual Report (1959); Riordan (1958, 1956b)]' Phillips Petroleum Company [Pursglove (1961); Weaver (1963)] , Standard Oil of Ohio [Klingel and McIntyre (1962); Pappas(1962)], and Monsanto Company [Anonymous (1960); Hehner (1963c)]. Several applications in the food industry are also mentioned, in particular use by Swift and Company [Samuel (1962)], Canadian Packers Limited [Samuel(1962)], and the A. E. Stanley Manufacturing Company [Koleff (1963)]. Also discussed are uses of EVOP by the canning industry [Filice (1963)], and by the Maumee Chemical Company in such diverse projects as saccharin production, biocide for sea lampreys isatoic anhydride, anthranilic acid and benzotriazole processes [Anonymous (1963)]. Other applications are mentioned in the automotive industry where EVOP was applied to resistance welding of automotive sheet metal [Thomas and Webster (1960)] and other manufacturing operations [Thomas (1965)]. Among these applications a savings of several hundreds thousand dollars per year by the Chemstrand Corporation has been mentioned by F. S. Riordan (1958,1959b), and a savings of $250,000 per year for two products has been reported by H. O. Hehner (1963c) in the Monsanto Company. In the description of uses by R. E. DeBusk (1962) that EVOP was used in approximately 15 processes with a savings of from $15,000 to $50,000 per year per process.

Box and Draper (1969) have regarded EVOP as a simple but powerful statistical tool with wide application in industry. Their experience has long shown that statistical methods, sometimes quite sophisticated in character, can be of great value in improving the efficiency of laboratory and pilot-plant investigations made by specially trained chemists and engineers.

2.5 Scope of the Present Work

Since the details of the interactions between the '*angle of attack and length of winglet*' with '*enhancement of heat transfer and loss of pressure energy*' are not still clearly understood, there is a general agreement that more research on this subject is required.

In this present work, a detailed three-dimensional numerical model of the MAC Algorithm is used which is able to provide a clear understanding of the physics of the flow and heat transfer. With the numerical model full Navier-Stokes equations together with governing equations for energy have been solved in a rectangular channel with built-in winglet vortex generators. The present study is aimed at a numerical investigation of heat transfer enhancement in a channel with built-in winglet type vortex generators using EVOP technique combined with Multi-criteria Decision Making and Pareto Optimality concepts.

The objectives of study can be explicitly stated as below:

- To optimize the delta winglet geometry in the channel so as to enhance the heat transfer by 30 %, or more, than that of the plain channel.
- To optimize the *pressure drop* in the channel flows and keep it as close as possible to that of the plain channel flow.

For the present study, Reynolds number is 790 and Prandtl number is 0.7, for all the heat exchanger design evaluations.

3. Heat Exchanger Optimization Formulation

3.1 Problem Optimization by EVOP

For the optimization of the problem above, there are two input variables and two output variables. The input variables are the '*angle of attack*' and '*the length of the winglet*' (refer Figure 3.1 and Fig. 3.2).

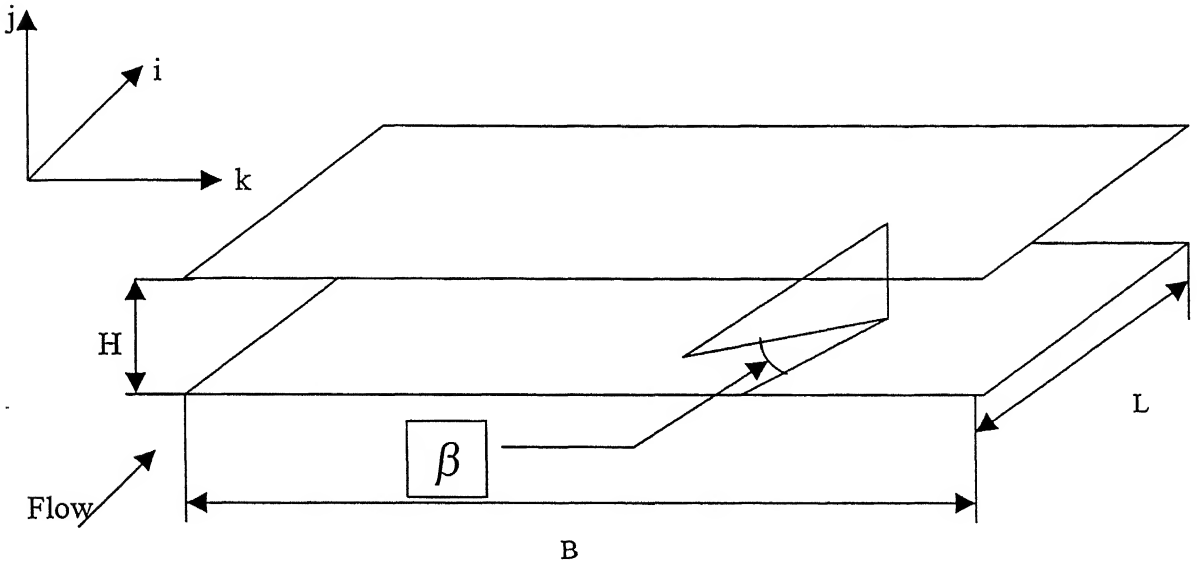

Figure 3.1: Geometry of Channel

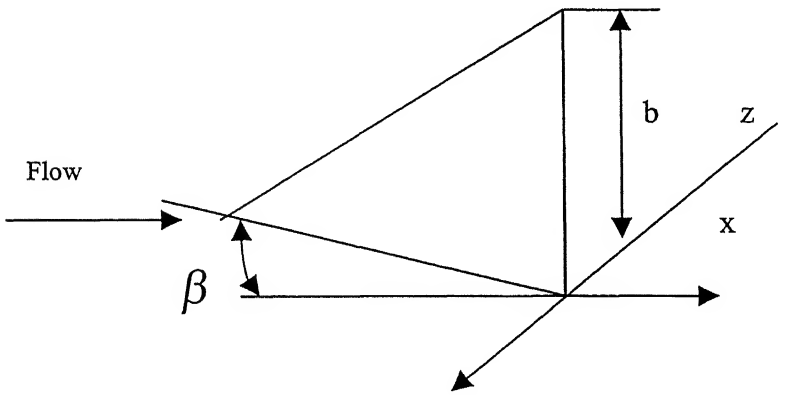

where,

B= width of channel, β = angle of attack, H= height of channel, l = length of winglet, L= length of channel, b = height of winglet

The two performance criteria that we wanted to optimize are 'Nusselt number' and 'Apparent friction factor'. For the EVOP technique, we calculated the average Nusselt number spanwise and further averaged it using 'Simpson's one third rule' of integration (Fig. 3.3). Thus, unique Nusselt number for each *angle of attack* with its respective length of winglet was calculated. This averaged Nusselt number was used as the measure of the heat transfer for the channel. Pressure drop was also calculated using average method. The pressure at the entry of the flow was calculated in the 'j' and 'k' directions and is averaged. The pressure at exit was also calculated and averaged. The difference between these two spanwise average pressures gives us the 'pressure drop'.

This 'pressure drop' was chosen as the second criterion for the optimization. So the task before us now was to optimize the input design variables, '*angle of attack*' and '*length of winglet*' in such a way that it would give us maximum Nusselt number while producing minimum pressure drop.

The EVOP discussed in the Chapter 1 can in general deal with 'n' number of input variables, but it takes into account the *single output parameter*, for optimization. The special feature of the present study is that, by varying the two input variables, vise '*angle of attack*' and '*length of winglet*', we maximize the response *Nusselt Number* while at the same time we are trying to keep the *pressure drop* as close as possible to that of a plain channel. To achieve this we employ 'Pareto Optimality' (Section 1.5) concepts.

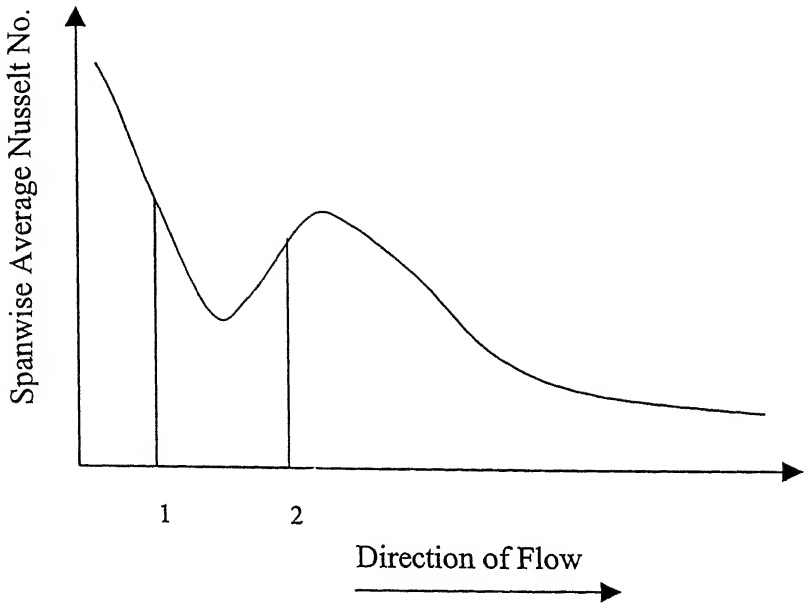

Figure3.3 (a): Symbolic Spanwise Average Nusselt Number Distribution

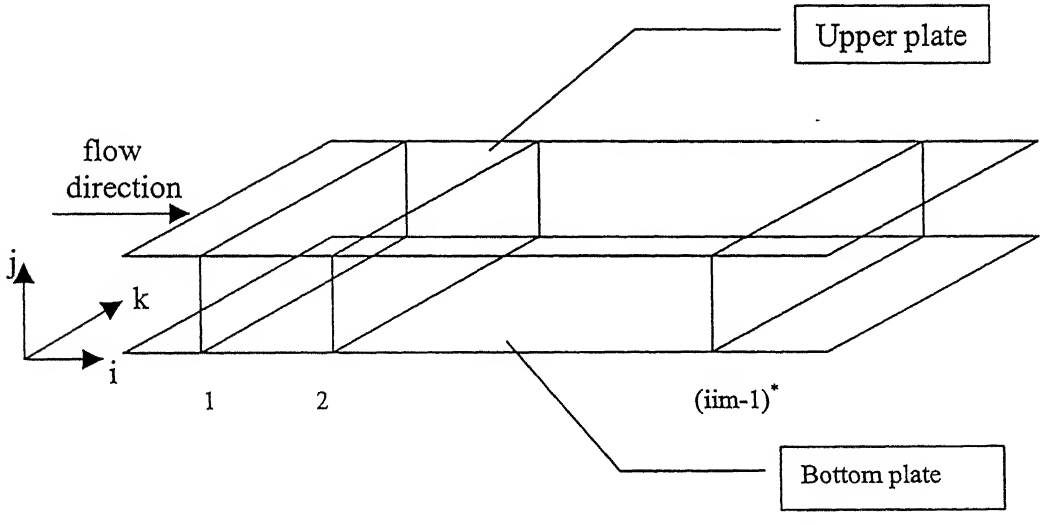

Figure 3.3 (b): Heat Exchanger with Upper and Bottom Plates showing cells in flow direction.

* iim is the total number of cells in the direction of flow. The first and last cell in the geometry are fictitious.

3.2 Methodology for Heat Exchanger Geometry Optimization

Let us consider Figure 3.4 as shown below. Here the Nusselt number is plotted on the X-axis, and the Pressure Drop is plotted on the Y-axis. The task ahead of us is to maximize Nusselt number, of the channel with winglet, while keeping the Pressure Drop as close as possible to that of the plain channel.

Let the points shown on the graph represent the outputs of the different runs for various 'angle of attacks' and 'length of winglet' (design variables) settings. Then from the figure we see that the points numbered 1,2, and 3 are representing the first 'Pareto front'. So, the neighborhood of these angles of attack and the length of winglet values are to be searched.

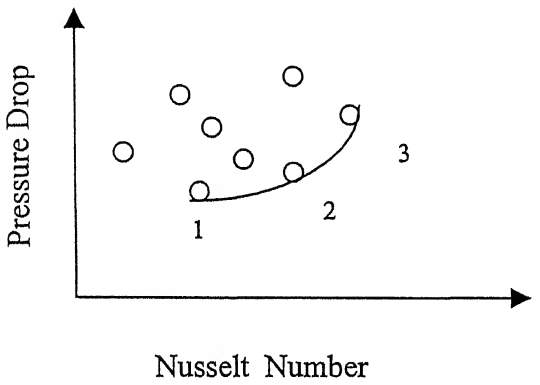

Figure3.4: Symbolic representation of Bi-criteria problem solutions in the Response Space

Suppose we take point '1' to start the EVOP study . Refer to Figure (3.5) below, which shows the four variants of point '1' namely 1a, 1b, 1c and 1d. In this figure, the angle of attack is shown on 'X' axis and the length of winglet is shown on 'Y' axis.

The same EVOP procedure is to be carried out for points 2 and 3. All new points are to be tested for the Pareto optimality. So, with the new inputs the process is run. These new inputs will give us new output values. The new output values are now again plotted on the graph to identify the members with Pareto property. (Figure 3.5)

The same procedure will be carried out for points 2 and 3 also. The new points obtained are tested for the optimality. So, with new inputs the process is ealuated. These new

inputs will give us new output values. The new output values are now again plotted on the bi-criteria response space.

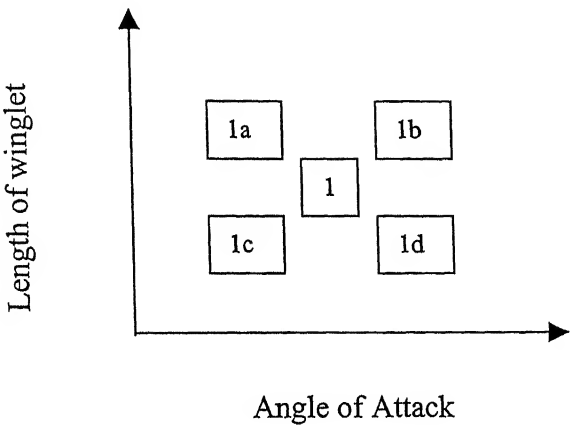

Figure3.5: Two dimensional variants in the Design Space

Refer to Figure (3.6) shown below.

By looking at the figure we see that a new (second generation) Pareto front consisting of 1d,2a,2b and 3a has emerged.

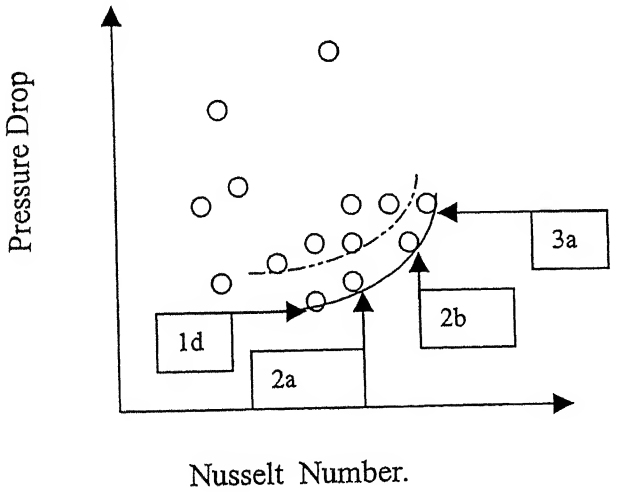

Figure3.6: New Pareto front in the Response Space after new input runs

The new Pareto front consists of points 1d, 2a, 2b and 3a. These points are plotted again on the 'angle of attack versus length of winglet' graph, and new EVOP variants are selected again and the process is re-run.

This process of plotting output and then selecting new input parameters accordingly is conducted iteratively, till the Pareto front is saturated and does not improve much. After *saturation* is reached, the series of input variable pairs representing the solution on the Pareto front will give us the set of optimal solutions, or input parameters.

We must point out here that the process of optimization involves the judgement of the designer. Thus the decision to fathom out some solution area or exclude some input from further searching is really subjective. So this process of EVOP-based design optimization would depend on experience, knowledge and the ingenuity of the designer himself.

3.3 Determination of Performance Parameters

Calculation of Optimization Parameters:

The Spanwise Average Nusselt number is calculated. Fig. 3.3(a) shows the symbolic curve for the Nusselt number distribution spanwise, along the direction of the flow i.e. I direction. To calculate the spanwise average of Nusselt number the following procedure is adopted:

- The Nusselt number at plane number 1 is calculated on bottom plate and is averaged on the 'K' direction.
- The Nusselt number at plane number 1 is calculated on upper plate and, is also averaged on the 'K' direction.
- Now, the average of these, bottom plate Nusselt number and the upper plate Nusselt number is calculated. This is spanwise average Nusselt Number.

Fig.3.3(a) shows the spanwise Nusselt number, at position '1', shown in Fig.3.3(b).

The area under curve shown in Fig. 3.3(a) is calculated using, Simpson's one-third rule of integration. The final Nusselt number, which is used as one of the optimizing objective, is calculated by averaging this area on the length of the channel in the direction of flow.

The pressure drop is calculated as follows:

- Spanwise average apparent friction is calculated at the entry of the heat exchanger, along the plane '1', where the node number is 2 in the flow direction.
- Spanwise average friction factor is calculated at the (iim-1)[1] plane.
- The subtraction of apparent friction factor at plane 1, and the apparent friction factor at plane (iim-1) will give us the value of the second objective of optimization.

[1] Where, iim is the total number of cells in the direction of the flow in the channel. The first and last cells are fictitious

4. Results and Analysis

4.1 Initial Solutions

4.1.1 Channel Geometry

EVOP technique specifically operates on improving process *after* its start-up. So to get started with initial solutions we must first of all fix up the geometry of the channel. Subsequently *optimization* will be carried out in a direction to enhance the *Average Nusselt Number* while maintaining the *pressure drop* to its minimum possible.

In selecting the Channel Geometry the dimensions are so chosen that it will accommodate a change in *length of winglet* up to 150%and a change in *angle of attack* from 0° to 90°.

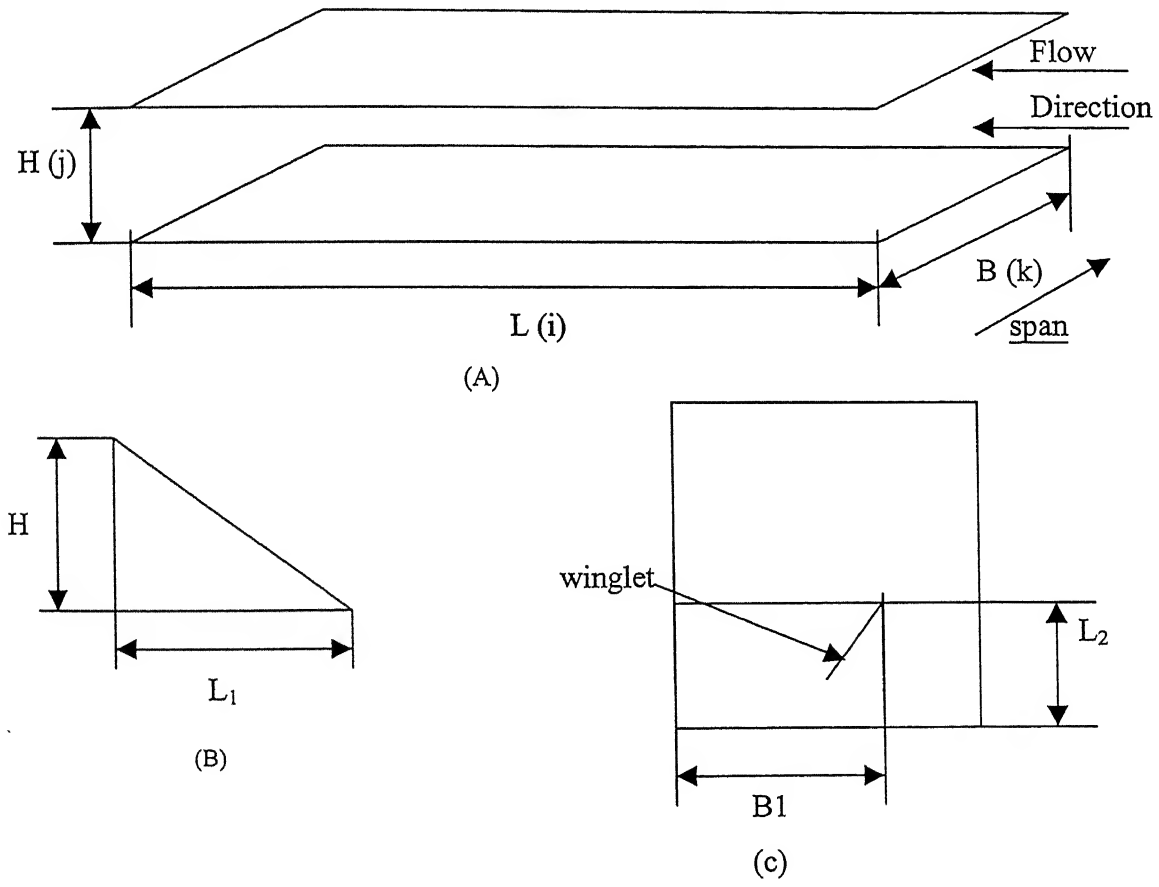

Figure (4.1): Channel Geometry: (a) Geometry of heat exchanger plates (b) Geometry of winglet (c) Top view of the winglet on heat-exchanger plate

The following dimensions were used in the numerical investigations of this study:

$B = 4.0$, $L = 11.5$, $H = 1.0$, $L_1 = 2.5$ (variable), $L_2 = 4.0$, $B_1 = 3.0$

The purpose behind choosing this kind of geometry was that by fixing the trailing edge position of the winglet, any changes in the angle of attack and the length of winglet could be accommodated. This will lead to draw a fair conclusion about the effects of inputs on the outputs, and the decision making task could be eased.

As shown in Figure 4.1, all the dimensions related to Channel and the position of the trailing edge of the winglet are fixed.

4.1.2 Sample Calculations for determining Input Parameters for MAC (Marker and Cell) Algorithm

The inputs to the MAC algorithm for numerical run are calculated as shown below. For demonstrating the sample calculation the *angle of attack* is chosen equal to 30° and the *length of winglet* is chosen equal to 2.5.

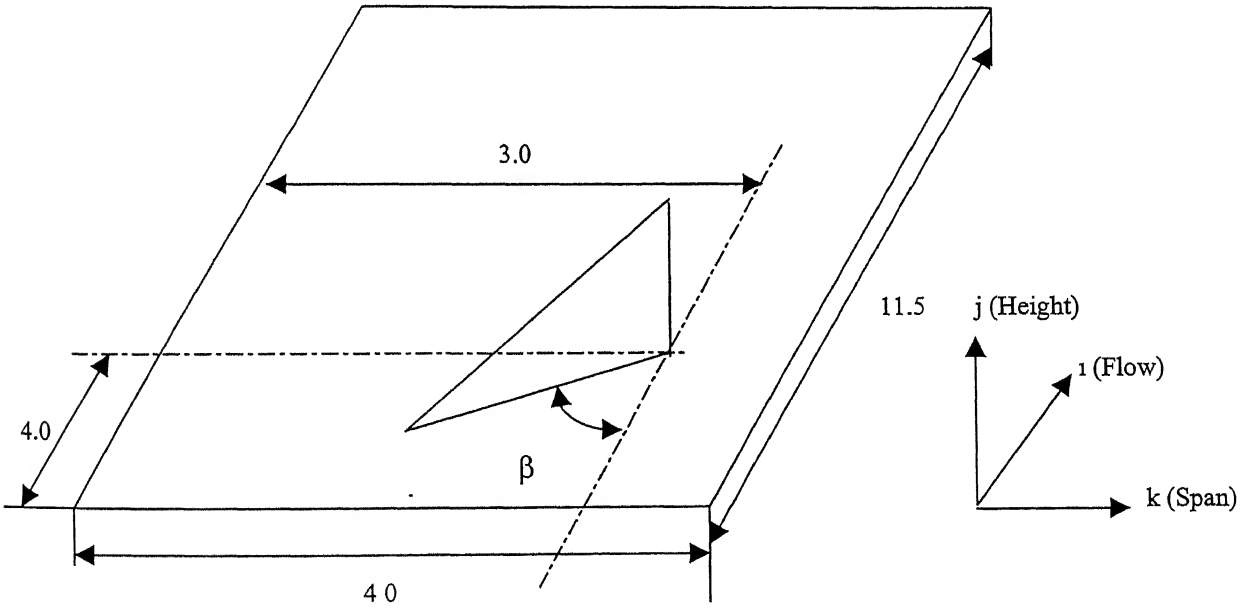

Figure 4.2: (a) Channel dimensions

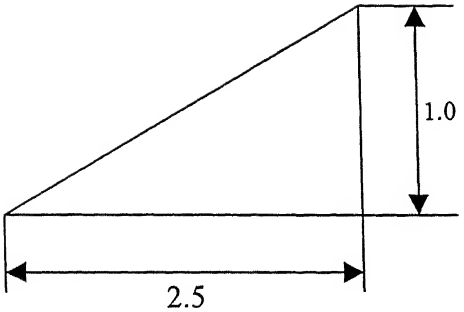

(b)

Figure (4.2): (b) Sample Winglet Dimensions

After fixation of the input parameters, the calculation of input parameters for MAC algorithm are carried out as shown below:

$f_y = 1.0$, $\Delta y = 0.05$, $\beta = 30°$, $H = 1.0$, $B = 4.0$, $L = 11.5$, $L_2 = 4.0$, $B_1 = 3.0$.

$$\Delta z = f_z * 0.05$$

$$f_z = L_1 * \sin \beta$$

$$\therefore f_z = 2.5 * \sin 30 = 1.25. \qquad (4.1)$$

from equation (4.1)

$$\Delta z = 1.25 * 0.05 = 0.0625 \qquad (4.2)$$

$$(jim-2) * \Delta y = H$$

$$\therefore jim = 22 \qquad (4.3)$$

$$\beta = \tan^{-1} (\Delta z / \Delta x)$$

$$\therefore \Delta x = (0.0625 / \tan 30) = 0.108 \qquad (4.4)$$

from equation (4.2)

$$B = (kim-2) * \Delta z = 4.0$$

$$\therefore kim = 66 \qquad (4.5)$$

from equation (4.4)

$$L = (iim-2) * \Delta x$$

$$\therefore iim = 108 \qquad (4.6)$$

$$kc = (B_1 / \Delta z) + 1$$

$$\therefore kc = 29 \qquad (4.7)$$

$$kb = \{(B_1 - L_1 \sin \beta) / (\Delta z)\} + 1$$

$$\therefore kb = 9 \qquad (4.8)$$

$$ib = (L_1 / \Delta x) + 1$$

$$\therefore ib = 37 \qquad (4.9)$$

$$H = \{(ib - ia)+1\} * \Delta y = 1.0$$

$$\therefore (ib - ia) = 19 \qquad (4.10)$$

from equation (4.9) and (4.10) we calculate,

$$\therefore ia = 19 \qquad (4.11)$$

where,

iim = total number of cells in 'i' direction. (flow)

jim = total number of cells in 'j' direction. (height)

kim = total number of cells in 'k' direction. (span)

kc = coordinate of trailing edge of winglet in 'k' direction.

kb = coordinate of leading edge of winglet in 'k' direction.

ib = coordinate of trailing edge of winglet in 'i' direction.

ia = coordinate of leading edge of winglet in 'i' direction.

Finally, the values of iim, jim, kim, fx, fy, fz, kb, ia and ib are the inputs to MAC algorithm. The procedure elaborated above, is carried out for every new input *angle of attack* and *length of winglet.*

$$L = (iim-2) * \Delta x$$

$$\therefore iim = 108 \qquad (4.6)$$

$$kc = (B_1 / \Delta z) + 1$$

$$\therefore kc = 29 \qquad (4.7)$$

$$kb = \{(B_1 - L_1 \sin \beta) / (\Delta z)\} + 1$$

$$\therefore kb = 9 \qquad (4.8)$$

$$ib = (L_1 / \Delta x) + 1$$

$$\therefore ib = 37 \qquad (4.9)$$

$$H = \{(ib - ia)+1\} * \Delta y = 1.0$$

$$\therefore (ib - ia) = 19 \qquad (4.10)$$

from equation (4.9) and (4.10) we calculate,

$$\therefore ia = 19 \qquad (4.11)$$

where,

iim = total number of cells in 'i' direction. (flow)

jim = total number of cells in 'j' direction. (height)

kim = total number of cells in 'k' direction. (span)

kc = coordinate of trailing edge of winglet in 'k' direction.

kb = coordinate of leading edge of winglet in 'k' direction.

ib = coordinate of trailing edge of winglet in 'i' direction.

ia = coordinate of leading edge of winglet in 'i' direction.

Finally, the values of iim, jim, kim, fx, fy, fz, kb, ia and ib are the inputs to MAC algorithm. The procedure elaborated above, is carried out for every new input *angle of attack* and *length of winglet*.

4.1.3 Calculation of Output (Response) Parameters

EVOP, would require responses, Nusselt number and pressure drop to be single-valued outputs for a particular angle of attack and length of winglet given as inputs. This was determined as follows.

For the calculation of pressure drop the spanwise averaged apparent friction factor was used. The difference between the spanwise averaged apparent friction factor at flow entry and that at flow exit was calculated which provided us the pressure difference between entry and exit. This is called the "pressure drop" throughout the current optimization process. For comparison, the pressure dro without any winglet is 0.01 (in the apparent friction factor scale).

For the calculation of average Nusselt number, first from MAC algorithm spanwise average Nusselt number at every cell along the flow direction was calculated. This gives us the spanwise distribution of average Nusselt number. In order to reach to a single unique number, Simpson's one-third rule of integration was used. (The detailed discussion of calculation of input and output parameters is done in Chapter 3.) In order to achieve this, separate code was written and was included in the post-processing code for MAC algorithm.

4.1.4 First phase of EVOP

To get started with the length of winglet, L_1 was chosen to be equal to 2.5. We treated the MAC algorithm as a 'Batch Process', in which two process variables or factors could be manipulated. These two factors are the *angle of attack* and the *length of winglet.* In order to generate a set of

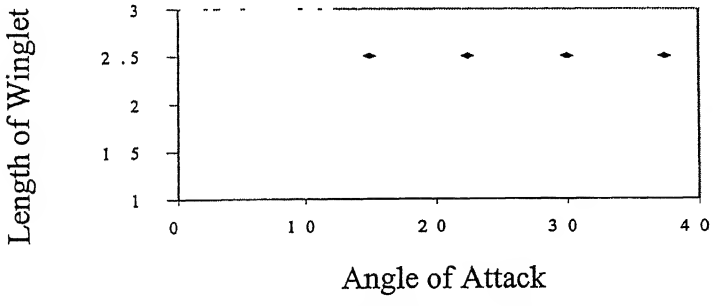

Figure 4.3: EVOP Table for Initial Runs in the input space

solutions, the length of winglet was fixed at 2.5, and by changing the *angle of attack* wise 15°, 22.5°, 30°, 37.5° the numerical runs were carried out.(We note that each of these MAC runs took

over 3 hours on the SGI Origin 2000 system.) The EVOP table for this initial set of inputs is shown in Figure 4.3.

After the initial set of numerical runs were conducted, we got the two responses as shown in Figure 4.4, in which *Nusselt Number* is plotted on X-axis and the *Pressure Drop* is plotted on the Y- axis. This gives us the initial set of solutions. These solutions were treated as the starting points for the EVOP optimization.

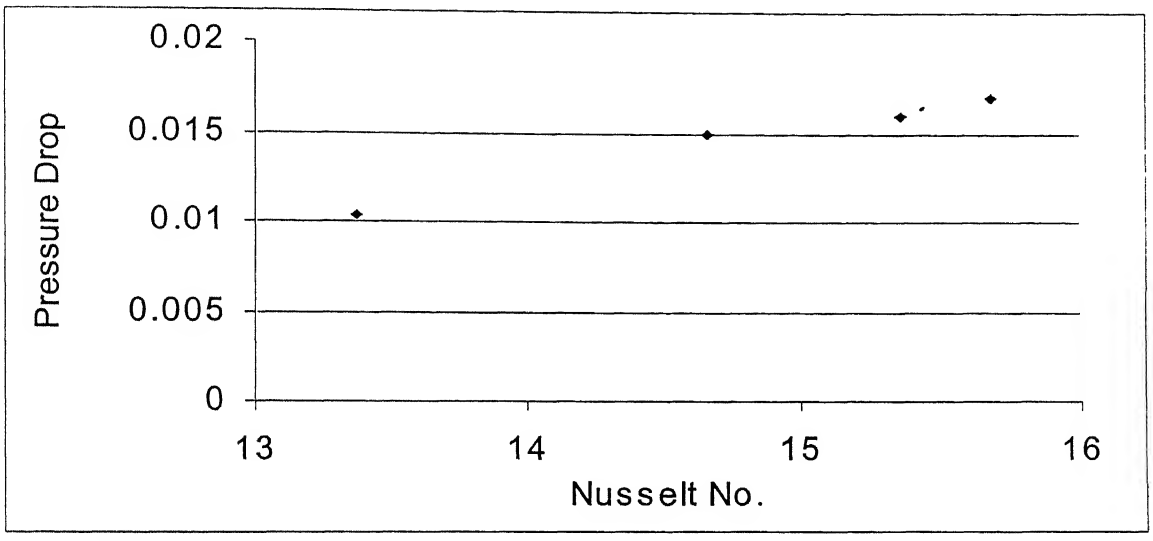

Figure 4.4: Initial Performance

Based on these outputs we have to take the decision regarding the next EVOP runs, in order to go in a direction of optimizing them.

4.2 Decision Making with EVOP

From the 'Information Board' (i.e. Fig. (4.4)) we see an useful pattern emerging from the increment in angle of attack while the length of winglet was held constant. The increment in angle of attack improved the *Average Nusselt Number*, but at the same time, it also increased the *pressure drop*. So, to get a picture of what a change in *length of winglet* brought about, we ran the MAC algorithm again for same angles of attack in the first phase of EVOP. But this time, the

length of winglet was increased up to its maximum feasible length in this particular chosen geometry of channel.[1]

By changing the length from $L_1 = 2.5$, to $L_1 = 3.75$ in the second phase of EVOP, the numerical runs were carried out at the angles of attack 15°, 22.5°, 30° and 37.5° respectively. Fig. 4.5 (a)

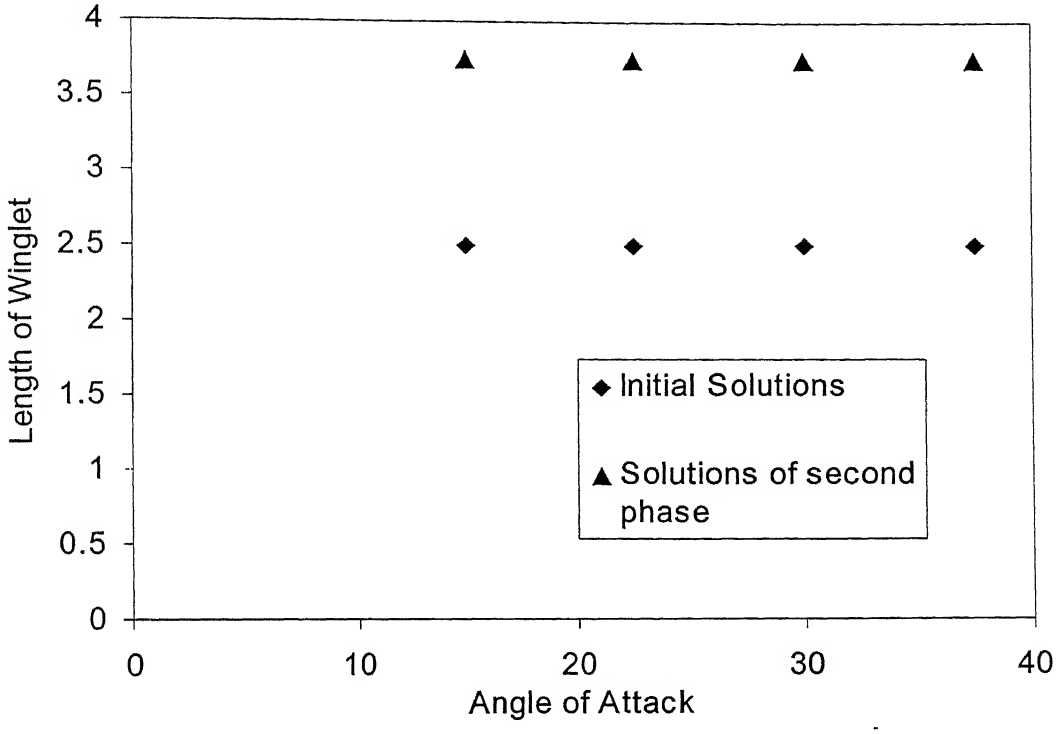

Figure 4.5 (a) EVOP table for second phase

shows the EVOP table for second phase. And Fig. 4.5(b) shows the result table for after the numerical run with second phase of EVOP.

From the 'Result Table' in Fig. 4.5(b) we infer that, increase in the *length of winglet* also has the same impact on the pressure drop. And also we can see that though the pressure drop has increased over the first phase runs, the Nusselt Number also has increased by a considerable margin. So, from this behavior we can conclude that by increasing angle of attack or the length of winglet we are going to get higher *Average Nusselt Number* accompanied by increased *Pressure Drop*.

[1] The channel geometry is designed in such a manner that, it can accomodate 150% change in length of winglet, that was used in the initial runs.

Next we explore the effect of reduction in the length of winglet for the set of angle of attack

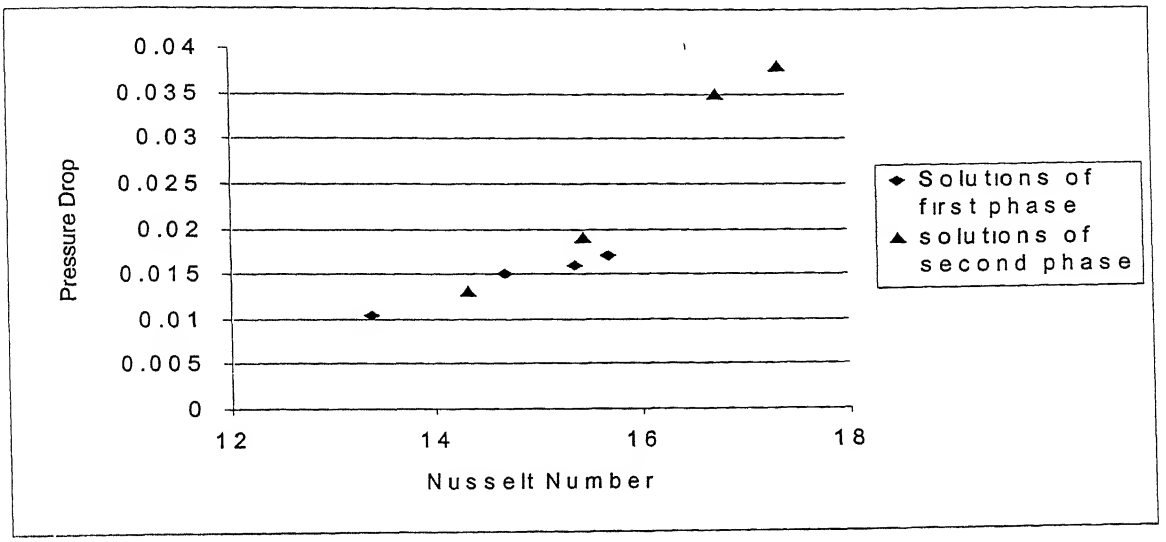

Figure 4.5 : (b) Results after second phase of EVOP

in initial set of numerical runs. We would expect (before the actual numerical runs are carried out), that the pressure drop will be lower and the average Nusselt number also will be lower than for

the set of inputs in the initial runs, if we decrease the length below 2.5. As we have fathomed out

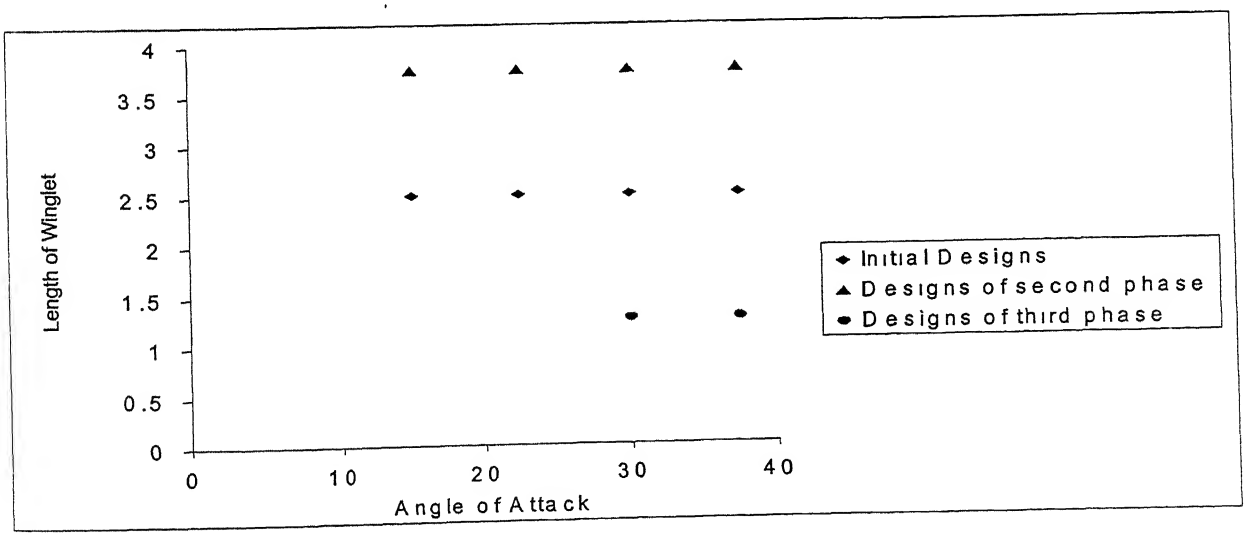

Figure 4.6: (a) Table for 3rd phase of EVOP

the upper limit of the length of winglet, we shall now also fathom out the lower limit of the

same. So arbitrarily we chose the length of wiglet to be equal to 1.25 (i.e. 50% of that of the initial inputs). As from the previous two phases of EVOP we can see that 15° angle of attack is not giving us any promising results, we eliminated it in this run, and the input angles of attack that we chose for third phase were 30° and 37.5°. The new EVOP table is as shown in Fig. 4.6(a). And the Result Table is shown in Fig. 4.6(b). From the Result Table we see that, the pressure drop for these new runs (marked by triangles) has decreased drastically and also the Nusselt number has decreased. Both the points are dominated by point '1'.

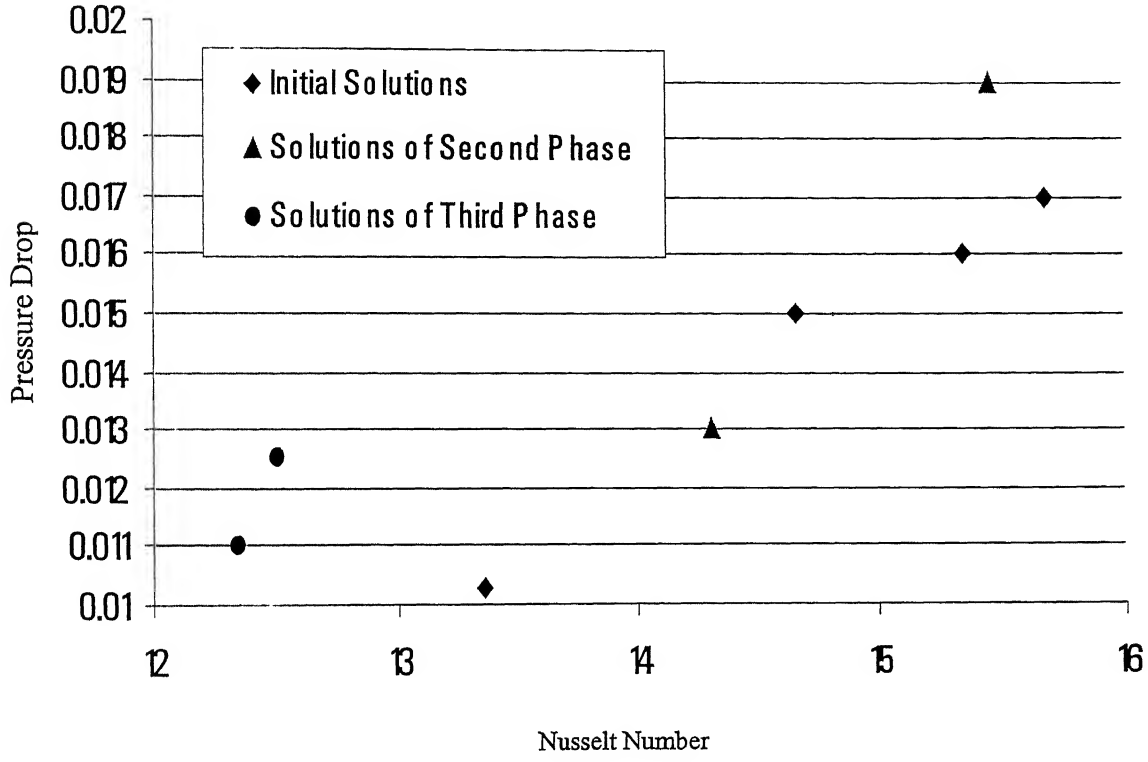

Figure 4.6: (b) Results after 3rd phase of EVOP

The Results after third phase are summarized in the Table 4.1.

4.3 Analysis of Solutions

As the three phases are over we now have established the relationship among input parameters, *angle of attack* and the *length of winglet* with the output parameters wise *Average Nusselt number* and the *Pressure drop.* At this stage we have to decide on the further input sets in order to go in a direction towards the objectives of EVOP optimization. To take the decision about it, Pareto Diagram was plotted as shown in Fig. 4.7, which shows the Pareto Diagram with separately indicating the set of Pareto solutions so far. These solutions are picked out for the further decision of new input sets.

Angle of Attack	Length of Winglet	Nusselt Number	Pressure Drop
15	2.5	13.37	0.0103
22.5	2.5	14.66	0.015
30	2.5	15.35	0.016
37.5	2.5	15.68	0.017
15	3.75	14.31	0.013
22.5	3.75	15.45	0.019
30	3.75	16.76	0.035
37.5	3.75	17.34	0.038
30	1.25	12.34	0.011
37.5	1.25	12.49	0.0125

Table 4.1: Summary of results after 3rd phase of EVOP

Table 4.2 enlists the Pareto solutions shown in Fig. 4.7.

After studying the graph shown in Fig. (4.7), we have decided not to fathom out the angles of attack wise, 15° and 22.5°. The reason for not fathoming 15° anymore is, for the largest length of winglet also, the Nusselt number is not improving much. And for the other lengths of winglet, the Nusselt number for 15° angle of attack, will lie somewhere below the 15° and 3.75 winglet length point on the result table. The reason for discarding 22.5° angle of attack is that, the output of 22.5° angle of attack with winglet length 3.75, is dominated by other points. And there is no need to fathom out this angle of attack further, as the Nusselt number is not going to improve further as well.

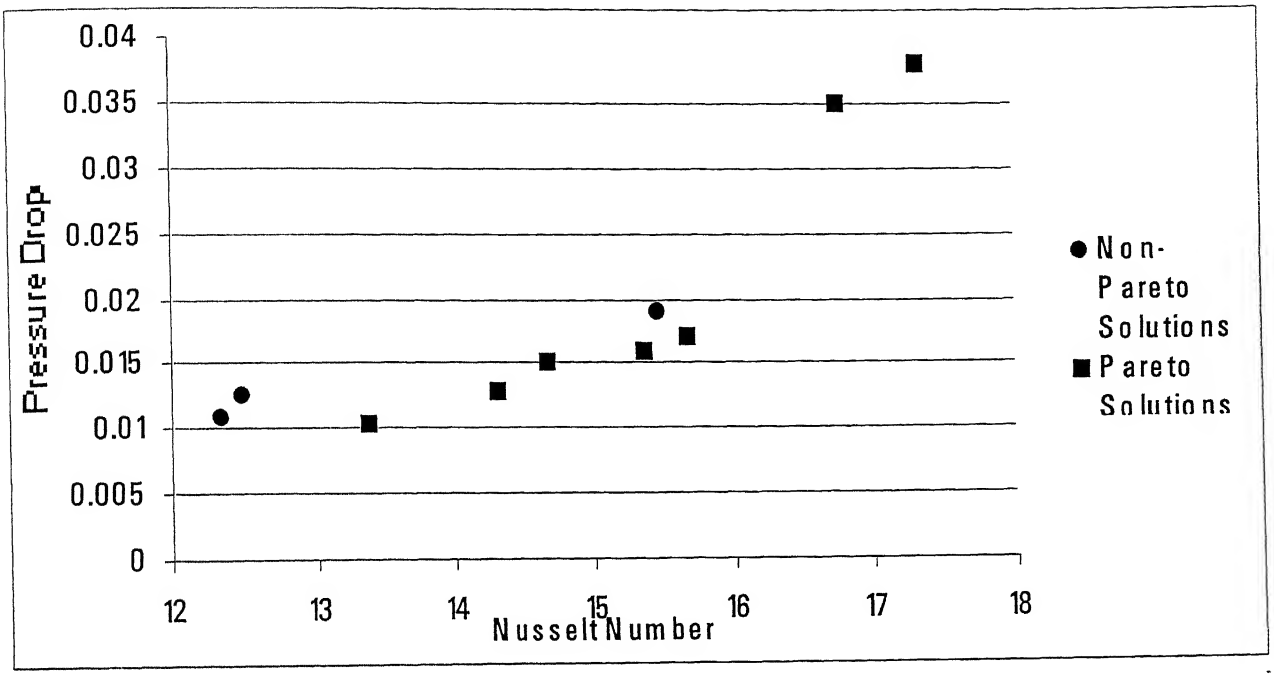

Figure 4.7: Pareto Solutions

Angle of Attack	Length of Winglet	Nusselt Number	Pressure Drop
22.5	2.5	14.66	0.015
37.5	2.5	15.68	0.017
37.5	3.75	17.34	0.038
30	3.75	16.76	0.035
30	2.5	15.35	0.016
15	3.75	14.31	0.013
15	2.5	13.37	0.0103

Table 4.2: List of Pareto Solutions after 3rd phase

We plotted EVOP table for these solutions. (Refer Fig. 4.8(a) to Fig. 4.8(e)) These EVOP tables have now evolved the further input sets which we have to fathom out in the 4th phase of EVOP. Table 4.3 enlists the new set of design inputs for the 4th phase. The decision of substitution of older input variables with the new input variables has been taken intuitively.

This new set of design inputs was fathomed out for its Pareto optimality by running the MAC algorithm with these inputs.

The procedure, that is explained above, for the determination of the new set of input variables was carried out iteratively. The final set of Pareto Solutions is to be fathomed further.

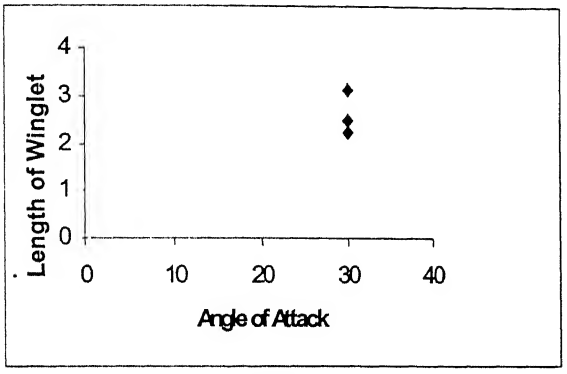

(a)

Variation introduced for 30° angle of attack

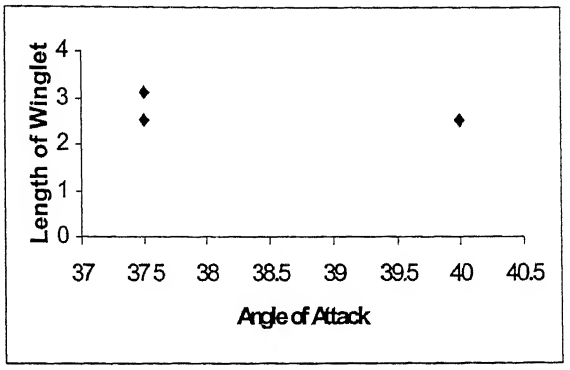

(b)

Variation introduced for 37.5° angle of attack

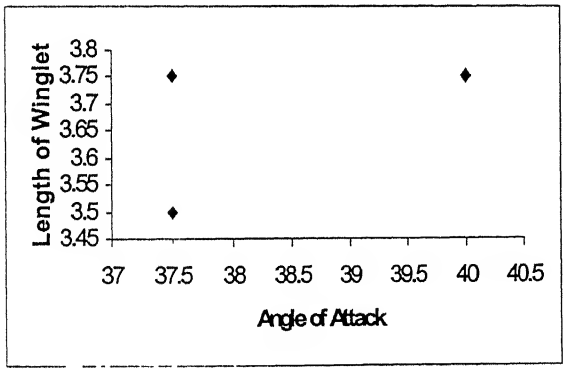

(c)

Variation introduced for 37.5° Angle of Attack

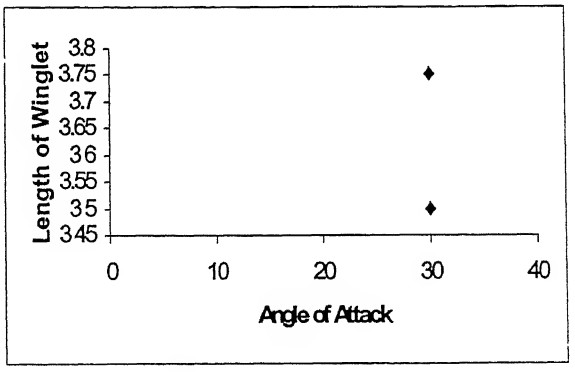

(d)

Variation introduced for 30° angle of Attack

Figure 4.8: EVOP Table for determination of Input sets of 4th phase

Angle of Attack	Length of Winglet
40	2.5
37.5	3.125
37.5	3.5
40	3.75
30	2.25
30	3.125
30	3.5

Table 4.3: Set of new inputs for 4th phase of EVOP

4.1 Results of EVOP Optimization

EVOP optimization was run iteratively and the final set of optimal solutions was reaached. In deciding the optimality, the lower bound on the Nusselt number was considered to be 15. According to this condition the optimal set of solutions was marked. Figure 4.9 shows the output of all the runs that were run for the optimization process, and Figure 4.10 shows the EVOP Diagram for the entire optimization process. The Pareto optimal solutions are also marked in fig.(4.11) and fig.(4.10).

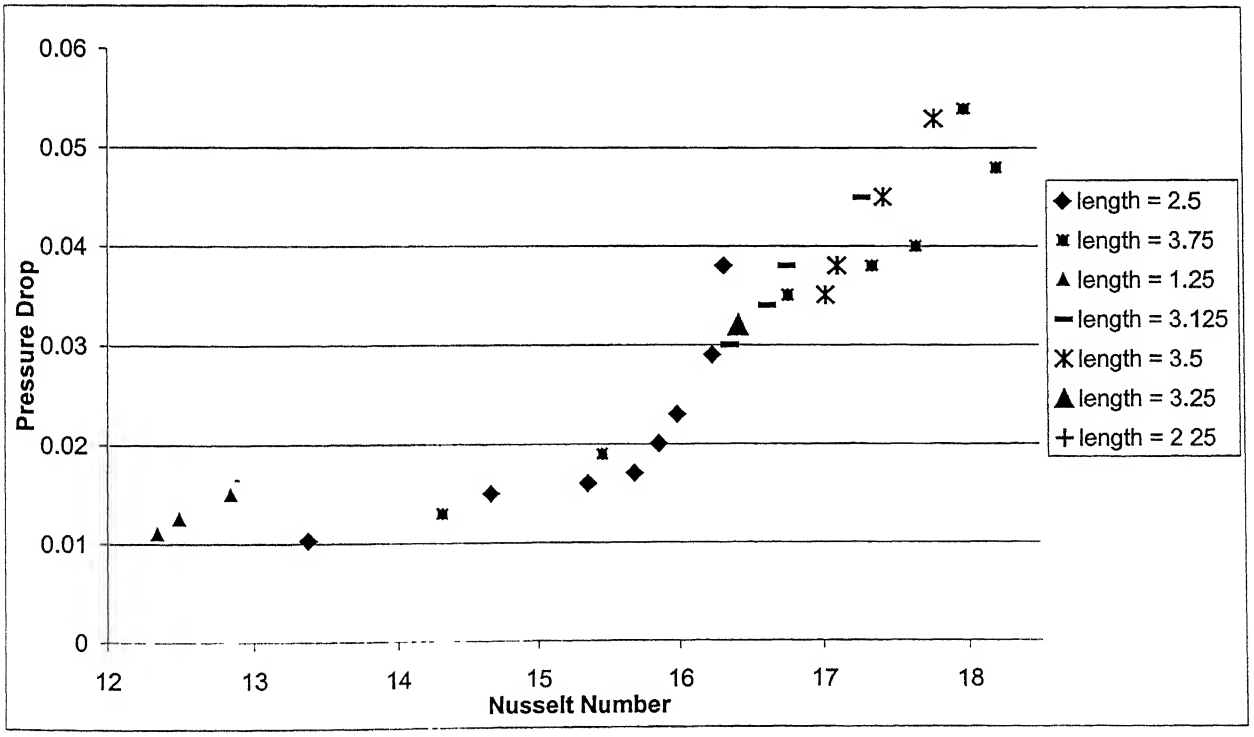

Figure 4.9: Output of all Evaluations

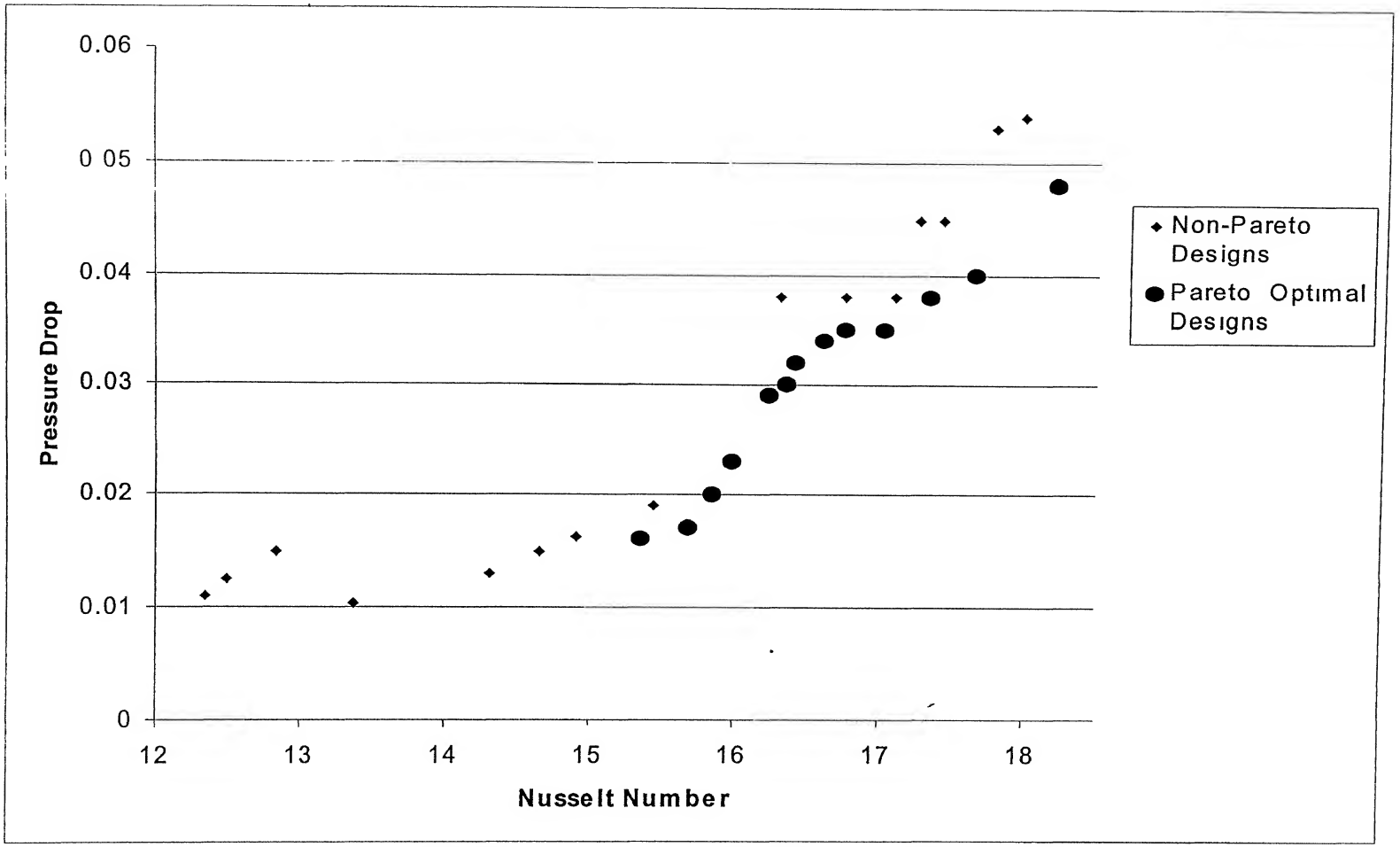

Figure 4.10: Pareto Optimaland Non-Pareto Design outputs

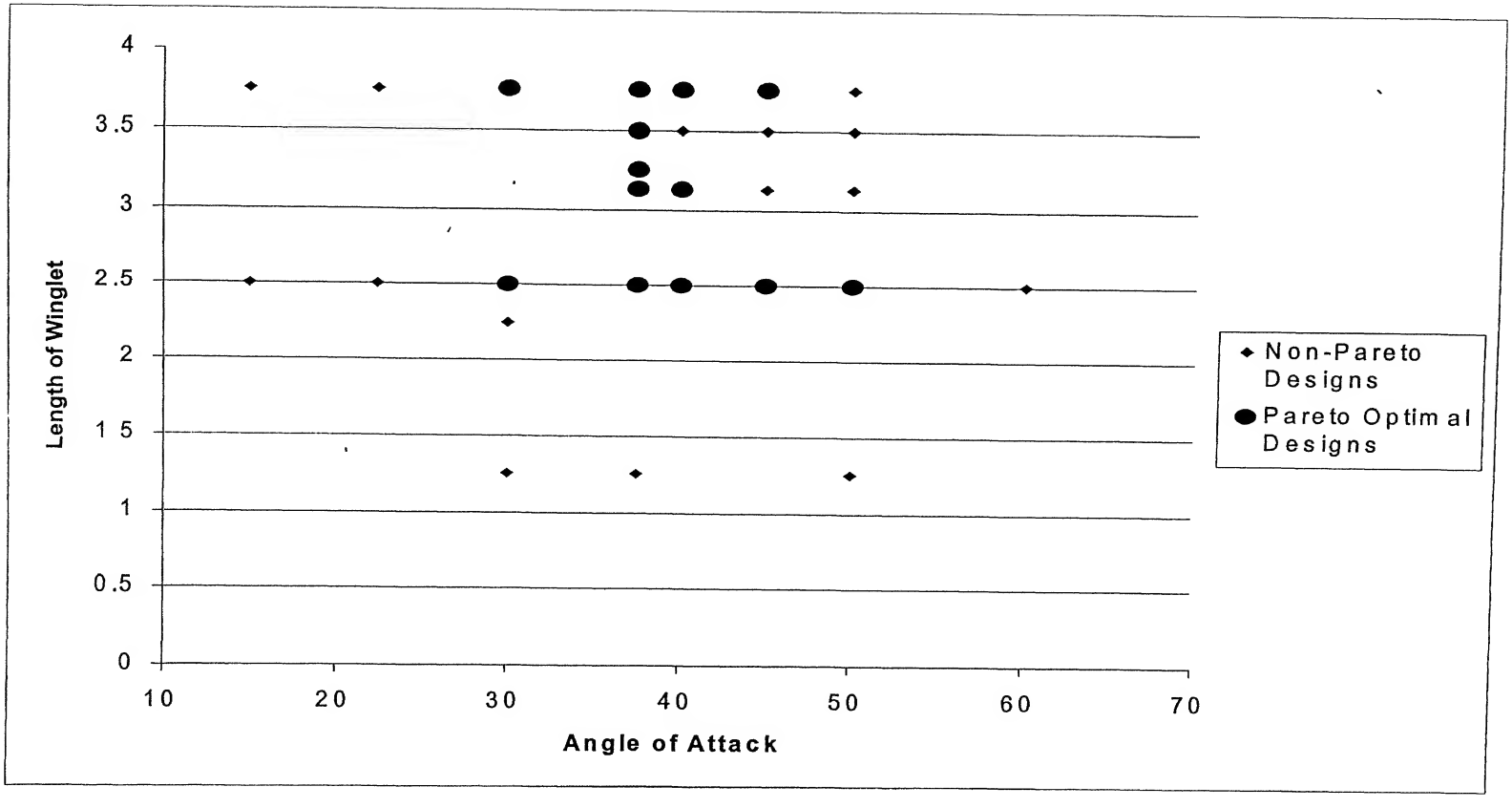

Figure 4.11: EVOP Table for Pareto Optimal and Non-Pareto designs

Table 4.4 shows the input as well as output of the runs that were carried out till including the last iteration.

From the fig. 4.9, we can easily find out the Pareto solutions. The Pareto optimal points are marked and are shown in the fig. 4.10. And the list of Pareto optimal points, stating their inputs as well as outputs is shown in Table 4.5.

From Table 4.5, fig. 4.10 and fig. 4.11, it can be inferred that the Pareto optimal solutions are mainly consisting of the angles of attack around 30° and 37.5°. And the optimal points are different combinations of these angles with length of winglet starting from 2.5 to 3.75.

Design Inputs			Design Outputs	
Design No.	Angle of Attack	Length of Winglet	Nusselt Number	Pressure Drop
1	15	2.5	13.37	0.0103
2	22.5	2.5	14.66	0.015
3*	30	2.5	15.35	0.016
4*	37.5	2.5	15.68	0.017
5*	40	2.5	15.85	0.02
6*	45	2.5	15.98	0.023
7*	50	2.5	16.23	0.029
8	60	2.5	16.31	0.038
9	15	3.75	14.31	0.013
10	22.5	3.75	15.45	0.019
11*	30	3.75	16.76	0.035
12*	37.5	3.75	17.34	0.038
13*	40	3.75	17.65	0.04
14*	45	3.75	18.2	0.048
15	50	3.75	17.98	0.054
16	30	1.25	12.34	0.011
17	37.5	1.25	12.49	0.0125
18	50	1.25	12.84	0.015
19*	37.5	3.125	16.35	0.03
20*	40	3 125	16.61	0.034
21	45	3.125	16.75	0.038
22	50	3.125	17.27	0.045
23*	37.5	3.5	17.02	0.035
24	40	3.5	17.1	0.038
25	45	3.5	17.42	0 045
26	50	3.5	17.78	0.053
27*	37.5	3.25	16.41	0.032
28	30	2.25	14.9	0.0163

Table 4.4: Input and Output of all the Designs

In Table 4.4 , the Pareto solutions are marked separately.

Design Inputs			Design Outputs	
Design No.	Angle of Attack	Length of Winglet	Nusselt Number	Pressure Drop
1	30	2.5	15.35	0.016
2	37.5	2.5	15.68	0.017
3	40	2.5	15.85	0.02
4	45	2.5	15.98	0.023
5	50	2.5	16.23	0.029
6	30	3.75	16.76	0.035
7	37.5	3.75	17.34	0.038
8	40	3.75	17.65	0.04
9	45	3.75	18.2	0.048
10	37.5	3.125	16.35	0.03
11	40	3.125	16.61	0.034
12	37.5	3.5	17.02	0.035
13	37.5	3.25	16.41	0.032

Table 4.5: Input and Output of Pareto Optimal Winglet Designs

5. Conclusions

5.1 Technical Summary

5.1.1 Results of the Present Work

This study has appraised the utility of EVOP methods for deriving multiobjective solutions to engineering design problems, where GA or other methods cannot work due to practical limitations. This work illustrates that EVOP can be effectively used in such situations to find Pareto Optimal multi-objective engineering designs.

Table 5.1 displays example Pareto Optimal designs that were reached when optimization of channel geometry was attempted using the EVOP technique. These solutions shown possess Nusselt number between 15 and 18 roughly, while their pressure drop varies from 0.016 to 0.05.

Design Inputs			Design Outputs	
Design No.	Angle of Attack	Length of Winglet	Nusselt Number	Pressure Drop
1	30	2.5	15.35	0.016
2	37.5	2.5	15.68	0.017
3	40	2.5	15.85	0.02
4	45	2.5	15.98	0.023
5	50	2.5	16.23	0.029
6	30	3.75	16.76	0.035
7	37.5	3.75	17.34	0.038
8	40	3.75	17.65	0.04
9	45	3.75	18.2	0.048
10	37.5	3.125	16.35	0.03
11	40	3.125	16.61	0.034
12	37.5	3.5	17.02	0.035
13	37.5	3.25	16.41	0.032

Table 5.1: Final Set of Pareto Optimal Winglet Designs

5.1.2 Technical Conclusions

The technical inferences specific to the heat exchanger design studied, of the present work may be summarized as follows.

1. The *angle of attack* up to 22.5° does not provide us with considerable increment in Nusselt number as compared to larger *angles of attack*, though the pressure drop up to 22.5° *angle of attack* is much lower comparatively.
2. If we go for angles of attack larger than 40° then these designs show a large increment in pressure drop though there is increment in Nusselt number also.
3. If we go on increasing angle of attack, then at a certain point the Nusselt number reaches its maximum, and if the angle of attack is further increased beyond this point then it drops, and it is accompanied with larger pressure drop over previous angles of attack.
4. In the present study, it is observed that the angle of attack between 30° and 40° give better results with Nusselt number in between 15 to 18, with a pressure drop between 0.016 to 0.05 for the length of winglet between 2.5 to 3.75
5. If the length of winglet is decreased below 2.5 then although the pressure drop is much lower, the Nusselt number does not increase much. So, at a lower length than 2.5, there is a larger compensation for Nusselt number though pressure drop is improved somewhat.
6. If the length of winglet is increased beyond 3.5, the increment in Nusselt number is always accompanied with larger and larger pressure drops.
7. EVOP is a workable optimization technique for channel geometry decision making, as it can be used, in the present case, for calculating Nusselt number and Pressure drop in advance, and designing of the channel and obstacle body will be much more convenient. It is very helpful in the sense that there is scarcity of knowledge as to what effects do the obstacle geometry has on the heat transfer phenomena.

5.2 Overall Conclusions of the Present Work

5.2.1 Optimization Methods and EVOP

Evolutionary Operation has sometimes been referred to as an *optimization* technique and is compared with other optimization techniques. Such comparisons must be considered with some caution, for the following reasons.

Evolutionary Operation is an experimental technique for seeking the *preferable*. By contrast, problems of mathematical optimization are usually concerned with determining the maximum or minimum of some function $z = f(x_1,....,x_k)$ within some region $R(x_1,.....,x_k)$ of the space of the x's, where usually it is assumed that:

1. The variables $x_1,.....,x_k$ are known.
2. The region $R(x_1,.....,x_k)$ is known.
3. The nature of the function $z = f(x_1,....,x_k)$ is known.
4. The function $z = f(x_1,....,x_k)$ can be computed without error for any chosen set of x's.

The situation which is met when we attempt to improve any process using EVOP differs from the mathematical optimization setup in a number of respects:

1. We do *not* know the variables $x_1,....,x_k$ which should be included in the function f.
2. We do *not* know with exactitude the region $R(x_1,.....,x_k)$ in which we should seek to maximize z.
3. We do *not* know the functional form f.
4. The observations are usually subject to moderate or large errors.

5.2.2 Consequences of using EVOP

We may know, at any given stage of an EVOP investigation, that we have found conditions which are preferable to those previously considered. However we can rarely know that we have attained *best* conditions. Some of the reasons are as follows:

1. Even if a process existed where improvement of a single response such as yield was the only criterion, we would seldom know how far or short of this theoretical point was the practical maximum reached by EVOP.
2. In practice, the objective function will almost always need to take into account a *number* of responses such as yield, cost, and so on. It would be even less possible to be sure that the optimum objective had been attained when improvement was so many faceted. The Pareto concept may address static situation reasonably. However the importance of the various characteristics may change from time to time depending on the state of the market, the nature of competitive products, and so on. It is therefore extremely unlikely that we could ever be sure that the ultimate for a

multidimensional and shifting objective function of this kind had ever been achieved by EVOP.

Most importantly, in the typical EVOP situation we cannot say at any point that no new possibilities for improvement will become available. Thus, optimum to EVOP is like the pot of gold at the end of a rainbow.

5.3 Scope for Future Work

1. The present study has used MAC algorithm and it has been limited to numerical investigation only. By execution of the physical heat transfer process, the outcome of this present work may be validated. This will require an experimental setup and the actual experimentation with different geometries.

2. Some alternate, faster method than MAC algorithm, perhaps not as accurate, may be evaluated to broadly search the design space by EVOP before fine tuning by MAC algorithm is done.

3. The work is based on the EVOP technique. There are some methods like ROVOP (Rotating square Evolutionary Operation) and REVOP (Random Evolutionary Operations) and Simplex EVOP, which can also be used for the optimization of the same problem (Black and Draper (1969)). A comparative study may show which method is more efficient in optimizing the heat exchanger design geometry. This will reduce the efforts and time in the future for bi-criteria heat exchanger geometry design.

4. The present study has taken into account only two design variables viz. angle of attack and the length of winglet obstacle. In order to help the decision making of heat exchanger design, aspect ratio, i.e. the ratio of width of channel to the height of

channel, also can be taken as the third input variable. This will uncover the effect of aspect ratio on heat enhancement and pressure penalty. This may be more helpful to us and lead to much better heat exchanger geometries.

References

1. Adulbhan, P. and M. T. Tabucanon (1980). *"Multicriterion Optimization in Industrial Systems"*. Chapter 9, Decision models for industrial Systems Engineer and Managers, AIT, Bangkok, Thailand.

2. Bagchi, T. P. (1999). *Multiobjective Scheduling by Genetic Algorithms*, Kluwer

3. Box, G. E. P. and Draper, N. R. (1969), *"Evolutionary Operation: A Statistical Method for Process Improvement"*, John Wiley and Sons, Inc. New York.

4. Cochran, J. L. And M. Zeleny, eds, (1973) *"Multiple Criteria Decision Making"*, University of South Carolina Press.

5. Biswas, G., K. Torii, D. Fujii, K. Nishino *"Numerical and experimental determination of flow structure and heat transfer effects of longitudinal vortices in a channel flow"*, Int. J. Heat Transfer, Vol. 39, No. 16, pp. 3441-3451, 1996.

6. Biswas, G., (1995), Solution of Navier-Stokes Equations for Incompressible Flows Using MAC and SIMPLE Algorithms, in *Computational Fluid Flow and Heat Transfer,* ed. K. Muralidhar and T. Sundararajan, Narosa Publishing House, India.

7. Deb, K. And Srinivas, N(1995), *"Multiobjective Optimization using Nondimensional Sorting Genetic Algorithm"* MIT Press, Evolutionary Computations, 2(3), 221-248.

8. Holman, J. P., *"Heat Transfer"*, McGraw-Hill Book Company, Singapore, 1989.

9. Deb, Prashanta, (April, 1994), *"Three Dimensional Computation of Laminar and Turbulent Flows with Heat Transfer in a channel with Built-in Longitudinal Vortex Generators"*, PhD. Thesis, ME Department, IIT Kanpur.

10. Rao, P. Narayan (1999), *" Multiobjective Optimization of Injection Molding Process Parameters: A Study using Genetic Algorithms"*, M Tech. Thesis, IME, IIT Kanpur.

11. Srinivas, T. D. (1998) *"Multiple Criteria Optimization: An Evolution of Two Evolutionary Meta-Heuristic Methods"*, M Tech. Thesis, IME, IIT Kanpur.

12. Tabucanon, M. T. (1989) *"Multicriteria Decision Making in Industry"*, Elsevier Science Publishers, New York.